deconjugated in the cecum and colon to regenerate SN-38 through bacterial β-glucuronidase (34). In this study, CPT-11 was excreted into feces much more than NK012 and a high CPT-11 concentration was detected in the small intestinal epithelium. It is speculated that the highly excreted CPT-11 is reabsorbed in the small intestinal epithelium and converted to SN-38 to cause damage to the intestinal mucosa. On the other hand, NK012 was uniformly distributed in the mucosal interstitium at a lower concentration, which may be related to the less mucosal damage and diarrhea than those induced by CPT-11, although NK012 was observed for longer period than CPT-11. About other toxic effects including bone marrow, liver,

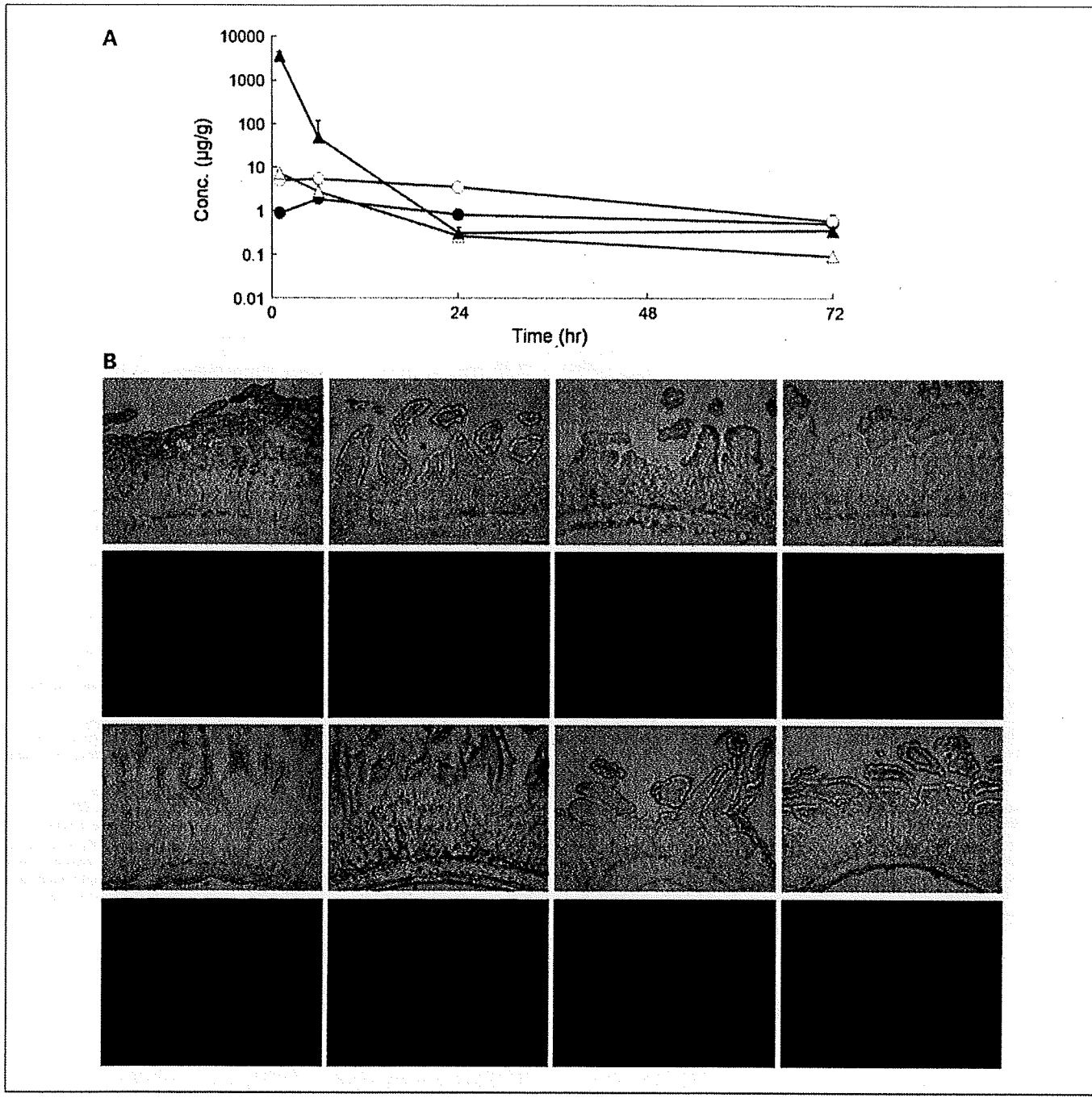

Fig. 4. Fecal concentrations of NK012, CPT-11, and free SN-38, and NK012 or CPT-11 distribution in the small intestine. *A*, distribution of NK012, CPT-11, and free SN-38 after i.v. administration of CPT-11 (30 mg/kg) or NK012 (20 mg/kg). ●, polymer-bound SN-38; ○, free SN-38 (polymer-unbound SN-38); Δ, SN-38 converted from CPT-11; ▲, CPT-11. *B*, small intestines were excised 1, 6, 24, and 72 h after i.v. administration of CPT-11 (30 mg/kg) or NK012 (20 mg/kg). Frozen sections were examined under a fluorescence microscope at a 358-nm excitation wavelength and a 461-nm emission wavelength. NK012 and CPT-11 were visualized as blue. The first or third columns are a bright-field image and the second or forth columns are a fluorescence image. Sections of small intestines were most well visualized in bright field. First, second, third, and fourth lines from the left side are images obtained 1, 6, 24, and 72 h after drug administration, respectively. CPT-11 was strongly distributed in the epithelium of the small intestine, whereas NK012 tended to be distributed weakly and uniformly in the mucosal interstitium.

and kidney toxicities, there was no significant difference between NK012/CDDP and CPT-11/CDDP in the present treatment schedule (data not shown).

In conclusion, NK012/CDDP showed a significantly higher antitumor activity with no severe diarrhea toxicity than CPT-11/CDDP, one of the most active regimens against SCLC and NSCLC. The present data suggest the clinical evaluation of NK012/CDDP in patients with SCLC and NSCLC.

Disclosure of Potential Conflicts of Interest

No potential conflicts of interest were disclosed.

Acknowledgments

We thank N. Mie and M. Ohtsu for their technical assistance and K. Shiina and K. Abe for their secretarial assistance.

References

1. Argiris A, Murren JR. Advances in chemotherapy for small cell lung cancer: single-agent activity of newer agents. Cancer J 2001;7:228–35.
2. Bodurka DC, Levenback C, Wolf JK, et al. Phase II trial of irinotecan in patients with metastatic epithelial ovarian cancer or peritoneal cancer. J Clin Oncol 2003;21:291–7.
3. Cunningham D, Pyrhonen S, James RD, et al. Randomised trial of irinotecan plus supportive care versus supportive care alone after fluorouracil failure for patients with metastatic colorectal cancer. Lancet 1998;352:1413–8.
4. Negoro S, Masuda N, Takada Y, et al. Randomised phase III trial of irinotecan combined with cisplatin for advanced non-small-cell lung cancer. Br J Cancer 2003;88:335–41.
5. Mathijssen RH, van Alphen RJ, Verweij J, et al. Clinical pharmacokinetics and metabolism of irinotecan (CPT-11). Clin Cancer Res 2001;7:2182–94.
6. Rothenberg ML, Kuhn JG, Burris HA III, et al. Phase I and pharmacokinetic trial of weekly CPT-11. J Clin Oncol 1993;11:2194–204.
7. Slatter JG, Schaaf LJ, Sams JP, et al. Pharmacokinetics, metabolism, and excretion of irinotecan (CPT-11) following i.v. infusion of [(14)C]CPT-11 in cancer patients. Drug Metab Dispos 2000;28:423–33.
8. Dvorak HF, Nagy JA, Dvorak JT, Dvorak AM. Identification and characterization of the blood vessels of solid tumors that are leaky to circulating macromolecules. Am J Pathol 1988;133:95–109.
9. Maeda H, Matsumura Y. Tumoritropic and lymphotropic principles of macromolecular drugs. Crit Rev Ther Drug Carrier Syst 1989;6:193–210.
10. Matsumura Y, Maeda H. A new concept for macromolecular therapeutics in cancer chemotherapy: mechanism of tumoritropic accumulation of proteins and the antitumor agent smancs. Cancer Res 1986; 46:6387–92.
11. Matsumura Y, Maruo K, Kimura M, Yamamoto T, Konno T, Maeda H. Kinin-generating cascade in advanced cancer patients and *in vitro* study. Jpn J Cancer Res 1991;82:732–41.
12. Koizumi F, Kitagawa M, Negishi T, et al. Novel SN-38-incorporating polymeric micelles, NK012, eradicate vascular endothelial growth factor-secreting bulky tumors. Cancer Res 2006;66:10048–56.
13. Nakajima TE, Yasunaga M, Kano Y, et al. Synergistic antitumor activity of the novel SN-38-incorporating polymeric micelles, NK012, combined with 5-fluorouracil in a mouse model of colorectal cancer, as compared with that of irinotecan plus 5-fluorouracil. Int J Cancer 2008;122:2148–53.
14. Sumitomo M, Koizumi F, Asano T, et al. Novel SN-38-incorporated polymeric micelle, NK012, strongly suppresses renal cancer progression. Cancer Res 2008;68:1631–5.
15. Saito Y, Yasunaga M, Kuroda J, Koga Y, Matsumura Y. Enhanced distribution of NK012, a polymeric micelle-encapsulated SN-38, and sustained release of SN-38 within tumors can beat a hypovascular tumor. Cancer Sci 2008;99:1258–64.
16. Eguchi Nakajima T, Yanagihara K, Takigahira M, et al. Antitumor effect of SN-38-releasing polymeric micelles, NK012, on spontaneous peritoneal metastases from orthotopic gastric cancer in mice compared with irinotecan. Cancer Res 2008;68: 9318–22.
17. Kuroda J, Kuratsu J, Yasunaga M, Koga Y, Saito Y, Matsumura Y. Potent antitumor effect of SN-38-incorporating polymeric micelle, NK012, against malignant glioma. Int J Cancer 2009;124:2505–11.
18. Fukuda M, Nishio K, Kanzawa F, et al. Synergism between cisplatin and topoisomerase I inhibitors, NB-506 and SN-38, in human small cell lung cancer cells. Cancer Res 1996;56:789–93.
19. Noda K, Nishiwaki Y, Kawahara M, et al. Irinotecan plus cisplatin compared with etoposide plus cisplatin for extensive small-cell lung cancer. N Engl J Med 2002;346:85–91.
20. Ohe Y, Ohashi Y, Kubota K, et al. Randomized phase III study of cisplatin plus irinotecan versus carboplatin plus paclitaxel, cisplatin plus gemcitabine, and cisplatin plus vinorelbine for advanced non-small-cell lung cancer: Four-Arm Cooperative Study in Japan. Ann Oncol 2007;18:317–23.
21. Ohe Y, Sasaki Y, Shinkai T, et al. Phase I study and pharmacokinetics of CPT-11 with 5-day continuous infusion. J Natl Cancer Inst 1992;84:972–4.
22. Masuda N, Fukuoka M, Kusunoki Y, et al. CPT-11: a new derivative of camptothecin for the treatment of refractory or relapsed small-cell lung cancer. J Clin Oncol 1992;10:1225–9.
23. Ohno R, Okada K, Masaoka T, et al. An early phase II study of CPT-11: a new derivative of camptothecin, for the treatment of leukemia and lymphoma. J Clin Oncol 1990;8:1907–12.
24. Kato K, Hamaguchi T, Shirao K, et al. Interim analysis of phase I study of NK012, polymer micelle SN-38, in patients with advanced cancer [abstract 485]. Proc Am Soc Clin Oncol 2008.
25. Burris III HA, Infante JR, Spigel DR, et al. A phase I dose-escalation study of NK012 [abstract 2538]. Proc Am Soc Clin Oncol 2008.
26. Natsume T, Watanabe J, Koh Y, et al. Antitumor activity of TZT-1027 (Soblidotin) against vascular endothelial growth factor-secreting human lung cancer *in vivo*. Cancer Sci 2003;94:826–33.
27. Chou TC, Talalay P. Quantitative analysis of dose-effect relationships: the combined effects of multiple drugs or enzyme inhibitors. Adv Enzyme Regul 1984; 22:27–55.
28. Kudoh S, Takada M, Masuda N, et al. Enhanced antitumor efficacy of a combination of CPT-11, a new derivative of camptothecin, and cisplatin against human lung tumor xenografts. Jpn J Cancer Res 1993;84: 203–7.
29. Hasegawa Y, Takanashi S, Okudera K, et al. Vascular endothelial growth factor level as a prognostic determinant of small cell lung cancer in Japanese patients. Intern Med 2005;44:26–34.
30. Giatromanolaki A, Koukourakis MI, Kakolyris S, et al. Vascular endothelial growth factor, wild-type p53, and angiogenesis in early operable non-small cell lung cancer. Clin Cancer Res 1998; 4:3017–24.
31. Ikuno N, Soda H, Watanabe M, Oka M. Irinotecan (CPT-11) and characteristic mucosal changes in the mouse ileum and cecum. J Natl Cancer Inst 1995;87: 1876–83.
32. Atsumi R, Suzuki W, Hakusui H. Identification of the metabolites of irinotecan, a new derivative of camptothecin, in rat bile and its biliary excretion. Xenobiotica 1991;21:1159–69.
33. Chu XY, Kato Y, Sugiyama Y. Multiplicity of biliary excretion mechanisms for irinotecan, CPT-11, and its metabolites in rats. Cancer Res 1997;57:1934–8.
34. Takasuna K, Hagiwara T, Hirohashi M, et al. Involvement of β-glucuronidase in intestinal microflora in the intestinal toxicity of the antitumor camptothecin derivative irinotecan hydrochloride (CPT-11) in rats. Cancer Res 1996;56:3752–7.

Cancer Therapy: Preclinical

Clinical Cancer Research

Antitumor Effect of NK012, a 7-Ethyl-10-Hydroxycamptothecin–Incorporating Polymeric Micelle, on U87MG Orthotopic Glioblastoma in Mice Compared with Irinotecan Hydrochloride in Combination with Bevacizumab

Jun-ichiro Kuroda[1,2], Jun-ichi Kuratsu[2], Masahiro Yasunaga[1], Yoshikatsu Koga[1], Hirotsugu Kenmotsu[1], Takashi Sugino[3], and Yasuhiro Matsumura[1]

Abstract

Purpose: To clarify the effect of bevacizumab on NK012 therapy in mice bearing U87MG glioblastoma orthotopic xenografts in comparison with the combination therapy of irinotecan hydrochloride (CPT-11) with bevacizumab.

Experimental Design: NK012 at 7-ethyl-10-hydroxycamptothecin (SN-38) equivalent dose of 30 mg/kg was administered intravenously three times every 4 days with or without bevacizumab. CPT-11 at 66.7 mg/kg was administered intravenously three times every 4 days or CPT-11 at 40 mg/kg/d over 5 consecutive days with or without bevacizumab. Bevacizumab was administered intraperitoneally six times every 4 days in each experiment. *In vivo* antitumor effects were evaluated by bioluminescence imaging, histopathologic evaluation, and immunohistochemistry. To evaluate interaction with bevacizumab, free SN-38 concentration in tumor tissues was examined by high-performance liquid chromatography.

Results: CPT-11 in combination with bevacizumab showed significantly more potent antitumor activity and longer survival than CPT-11 monotherapy ($P < 0.05$). However, there was no difference between NK012 monotherapy and NK012 in combination with bevacizumab. Concentration of free SN-38 released from NK012 in tumor tissue decreased in combination with bevacizumab ($P = 0.027$). NK012 monotherapy or NK012 with bevacizumab showed potent antitumor activity and longer survival than any dosing method of CPT-11 in combination with bevacizumab ($P < 0.05$). Orthotopic tumors treated with NK012 showed decreased tumor cellularity and lower Ki-67 index ($P < 0.001$) relative to those treated with CPT-11/bevacizumab.

Conclusions: The present study using orthotopic glioblastoma model in mice may warrant further preclinical evaluation of NK012 before conducting the clinical trial of the drug, because the antitumor activity of NK012 monotherapy was superior to the combination therapy of CPT-11 with bevacizumab.
Clin Cancer Res; 16(2); 521–9.

Malignant glioma, such as glioblastoma multiforme and anaplastic astrocytoma, are the most commonly occurring primary malignant brain tumors, and glioblastoma multiforme is well known as a typical hypervascular tumor with a high expression level of vascular endothelial growth factor (VEGF; ref. 1). Currently, glioblastoma multiforme patients have a mean survival time of only 50 weeks following the standard treatment consisting of surgical and adjuvant therapies (2). However, a recent phase III randomized trial for newly diagnosed glioblastoma multiforme showed that radiation therapy with concurrent temozolomide treatment followed by 6 months of temozolomide treatment was superior to radiation therapy alone in terms of overall survival (3). Furthermore, several clinical trials have shown that the median survival time of patients with recurrence was only 30 weeks (4). Therefore, a novel antitumor agent based on a new approach for the recurrent malignant glioma is eagerly awaited.

7-Ethyl-10-hydroxycamptothecin (SN-38) is a broad-spectrum anticancer agent targeting DNA topoisomerase I. Irinotecan hydrochloride (CPT-11), a prodrug of SN-38, shows some antitumor activity in patients with recurrent glioblastoma multiforme, with response rates of 0 to 17% in several trials (5–8). CPT-11 single-agent chemotherapy activity is thus similar to that of other agents used for

Authors' Affiliations: [1]Investigative Treatment Division, Research Center for Innovative Oncology, National Cancer Center Hospital East, Kashiwa, Japan; [2]Department of Neurosurgery, Faculty of Medical and Pharmaceutical Sciences, Kumamoto University, Kumamoto, Japan; and [3]Department of Pathology, Fukushima Medical University School of Medicine, Fukushima, Japan

Corresponding Author: Yasuhiro Matsumura, Investigative Treatment Division, Research Center for Innovative Oncology, National Cancer Center Hospital East, 6-5-1 Kashiwanoha, Kashiwa 277-8577, Japan. Phone: 81-4-7134-6857; Fax: 81-4-7134-6857; E-mail: yhmatsum@east.ncc.go.jp.

doi: 10.1158/1078-0432.CCR-09-2393

Translational Relevance

A recent phase II trial for recurrent glioblastoma multiforme showed that irinotecan hydrochloride (CPT-11) combined with bevacizumab is a promising and unprecedentedly effective treatment against the recurrent glioblastoma multiforme. However, there may be an increasing risk of developing venous thrombotic disease and intracranial hemorrhage with this combination therapy. The 7-ethyl-10-hydroxycamptothecin–incorporating polymeric micelle NK012 has been shown to have significant antitumor activity against several cancer mouse models compared with CPT-11. Two phase I trials in Japan and the United States showed that patients treated with NK012 did not develop grade 3/4 diarrhea, one of the major adverse effects of CPT-11. Here, NK012 showed potent antitumor activity and longer survival than CPT-11 in combination with bevacizumab in glioblastoma multiforme orthotopic tumor in mice. These results warrant clinical evaluation in patients with malignant glioma.

recurrent glioblastoma multiforme (7). Meanwhile, glioblastoma cells express high levels of VEGF *in situ*. Accordingly, antiangiogenic strategies may be a promising approach for malignant gliomas hypervascular in nature. A recent phase II trial for recurrent glioblastoma multiforme showed that CPT-11 combined with bevacizumab, an anti-VEGF monoclonal IgG1 antibody, is a promising and unprecedentedly effective treatment against the recurrent malignant glioma with a 6-month progression-free survival rate of 46% and a 6-month overall survival rate of 77% (9, 10). On the other hand, there may be an increased risk of developing venous thromboembolic disease and intracranial hemorrhage with this combination therapy. Therefore, it is reasonable to develop other available treatment modalities by which cytotoxic drugs can exert more potent antitumor activity to their full potential with modest adverse effects and thereby reasonably prolong the overall survival of recurrent glioblastoma multiforme patients.

NK012, a SN-38–incorporating polymeric micelle, is a prodrug of SN-38 similar to CPT-11. Polymer-conjugated drugs categorized under drug delivery system agents are favorably extravasated from tumor vessels into the interstitium of tumors due to the enhanced permeability and retention effect (11, 12). The enhanced permeability and retention effect is based on the following pathophysiologic characteristics of solid tumor tissues: hypervascularity; incomplete vascular architecture; secretion of vascular permeability factors stimulating extravasation within cancer tissue; and absence of effective lymphatic drainage from the tumors, which impedes the efficient clearance of macromolecules accumulated in solid tumor tissues. Moreover, macromolecules cannot freely leak out from normal vessels; thus, the adverse effect of an anticancer agent can be reduced. Very recently, we showed that NK012 exerted significantly more potent antitumor activity against several kinds of tumors including human glioma in xenograft models (13). In the present study, we report the antitumor activity of NK012 compared with CPT-11 combined with bevacizumab against orthotopic U87MG glioblastoma in nude mice.

Materials and Methods

Drugs. NK012 was supplied by Nippon Kayaku. Lyophilized NK012 was dissolved in sterile distilled water at a concentration of 5 mg/mL (SN-38 equivalent dose) just before administration to mice. The size of NK012 was ~20 nm in diameter with a narrow size distribution (12). CPT-11 was purchased from Yakult Honsha. Bevacizumab was purchased from Chugai Pharmaceutical.

Cell cultures. The human glioblastoma cell line U87MG was obtained directly from the American Type Culture Collection. A U87MG cell line clone stably expressing firefly luciferase named U87MG/Luc was established from polyclonal U87MG/Luc reported previously (13). The sensitivity of U87MG/Luc cells to NK012 and CPT-11 was almost similar to that of parental U87MG cells (data not shown). U87MG/Luc cells were maintained in DMEM supplemented with 10% fetal bovine serum (Cell Culture Technologies), penicillin, streptomycin, and amphotericin B (100 units/mL, 100 μg/mL, and 25 μg/mL, respectively; Sigma) in a humidified atmosphere containing 5% CO_2 at 37°C.

In vivo *orthotopic model and imaging.* Six- to 8-week-old female athymic BALB/c *nu/nu* mice (Charles River Japan) were used for this study. U87MG/Luc cells (5×10^5) suspended in 5 μL PBS were injected into the right frontal lobe of each mouse as described previously (13). *In vivo* bioluminescence imaging studies were done using the Photon Imager animal imaging system (BioSpace). For imaging, mice with intracranial U87MG/Luc tumor were simultaneously anesthetized with isoflurane, and D-luciferin potassium salt (Synchem) was intraperitoneally administered at a dose of 2.5 mg/mouse. For bioluminescence image analysis, regions of interest encompassing the intracranial area of a signal were defined using Photo Vision software (BioSpace), and the total number of photons per minute [counts/min (cpm)] was recorded. The pseudo-color luminescent image represented the spatial distribution of detected photon counts emerging from active luciferase within the animal. All animal procedures were done in compliance with the Guidelines for the Care and Use of Experimental Animals established by the Committee for Animal Experimentation of the National Cancer Center, Japan; these guidelines meet the ethical standards required by law and also comply with the guidelines for the use of experimental animals in Japan.

In vivo *tumor growth inhibition assay.* Eight days after inoculation of U87MG/Luc cells into the right hemisphere of the brain, mice with cpm >2,000 were randomly assigned into eight test groups of five mice

(2,296-15,624 cpm). After the randomization of mice based on cpm, we confirmed that the mean value of cpm was statistically identical between groups.

Treatment was started (day 0; Table 1). *In vivo* bioluminescence imaging was done by Photon Imager and luciferase activity was measured once a week (days 0, 7, 14, 21, 28, and 35). Body weight of each mouse of the treatment experiment was also measured once a week (days 0, 7, 14, 21, 28, and 35), and mortality and morbidity were checked daily from the day of treatment initiation. Simultaneously, to assess the survival of mice with intracranial U87MG/Luc tumor, mice were maintained until each animal showed signs of morbidity (20% weight loss and neurologic deficit), at which point they were sacrificed.

In all groups, the total dose of NK012 and CPT-11 was 90 mg/kg (SN-38 equivalent dose) and 200 mg/kg, respectively. A total dose of 200 mg/kg was shown previously to be the maximum tolerated dose (MTD) of CPT-11 in nude mice (14, 15). As CPT-11 is a schedule-dependent anticancer agent, it was administered under two different treatment regimens (16). Each drug was administered according to the mouse body weight: (*a*) normal 0.9% NaCl solution (q4d × 4, intravenously), (*b*) NK012 (30 mg/kg, q4d × 3, intravenously), (*c*) CPT-11 (66.7 mg/kg, q4d × 3, intravenously), (*d*) CPT-11 (40 mg/kg, qd × 5, intravenously), (*e*) bevacizumab (5 mg/kg, q4d × 6, intraperitoneally), (*f*) NK012 (30 mg/kg, q4d × 3, intravenously) with bevacizumab (5 mg/kg, q4d × 6, intraperitoneally), (*g*) CPT-11 (66.7 mg/kg, q4d × 3, intravenously) with bevacizumab (5 mg/kg, q4d × 6, intraperitoneally), or (*h*) CPT-11 (40 mg/kg, qd × 5, intravenously) with bevacizumab (5 mg/kg, q4d × 6, intraperitoneally) was administered to the mice (Table 1). In the case of combination therapy, drugs were administered concomitantly.

Evaluation of antitumor activity. The antitumor activity of each treatment was evaluated according to three criteria: (*a*) number of tumor regressions, (*b*) tumor growth delay, and (*c*) Kaplan-Meier analysis to determine the effect on the time to morbidity. Decrease >50% of the initial photon count (cpm) was defined as a tumor regression. It had to be observed for at least two consecutive photon-counting events to be retained. Tumor growth delay was defined as the difference in the median time to reach a photon count of 5-fold compared with that of day 0 between the treated group and the control group (14). To evaluate the change in photon count of each treatment group, repeated-measures ANOVA was carried out using the StatView 5.0 software package. $P < 0.05$ was regarded as significant. Statistical differences in the Kaplan-Meier curve of each group were ranked according to the Breslow-Gehan-Wilcoxon test using StatView 5.0.

Immunohistochemistry. Histologic sections were taken from U87MG/Luc orthotopic tumor tissues at day 15 from the initiation of each therapy. The time points for analysis were chosen according to when the best antitumor activity was obtained. The brain was removed from the skull, fixed in buffered 4% paraformaldehyde, embedded in paraffin, and then cut into 3-μm-thick sections. Conventional H&E-stained sections were prepared for general histopathologic evaluation. Immunohistochemistry was done using antibodies to human Ki-67 (BD Pharmingen), human VEGF (Santa Cruz Biotechnology), and mouse CD34 (MEC 14.7; Abcam). For antigen retrieval, sections were autoclaved in Dako REAL Target Retrieval Solution (Dako Denmark). Detection was done by Vectastain Elite avidin-biotin complex kit (Vector Laboratories) for CD34 and EnVision$^+$ system labeled polymer-horseradish peroxidase anti-mouse (DakoCytomation) for Ki-67 and anti-rabbit for VEGF. The proliferation index was evaluated by counting Ki-67$^+$ cells per 1,000 tumor cells using ImagePro Plus analysis software. VEGF immunoreactivity area was quantified using the analysis software BZ Analyzer (Keyence) with a constant color threshold in 10 high-power fields per slide (×400) and is given in percent of positive area in field of view. Tumor vascularity was assessed by counting CD34$^+$ microvessels in 10 high-power fields per slide (×400). The small intestine was sampled at 5 cm from the pylolic part for the jejunum and 5 cm

Table 1. Activity of three anticancer drugs against orthotopic U87MG xenografts

Treatment course	Dose (mg/kg/d)	Schedule	Total dose (mg/kg)	No. animals/ group	Maximum body weight loss (%)	Toxic death	Tumor regression	Tumor growth delay (d)	Median overall survival (d)
Control	—	—	—	5	—	—	—	—	29
NK012	30	q4d × 3	90	5	3.8	0	3	>18	48
CPT-11	66.7	q4d × 3	200	5	6.6	0	0	8	36
CPT-11	40	qd × 5	200	5	2	0	1	8	34
Bevacizumab	5	q4d × 6	30	5	1.9	0	0	4	40
NK012/bevacizumab	30/5	q4d × 3/q4d × 6	90/30	5	0.9	0	1	12	46
CPT-11/bevacizumab	66.7/5	q4d × 3/q4d × 6	200/30	5	0	0	2	7	40
CPT-11/bevacizumab	40/5	qd × 5/q4d × 6	200/30	5	0.7	0	2	8	41

NOTE: Maximum body weight loss (days 0-28).

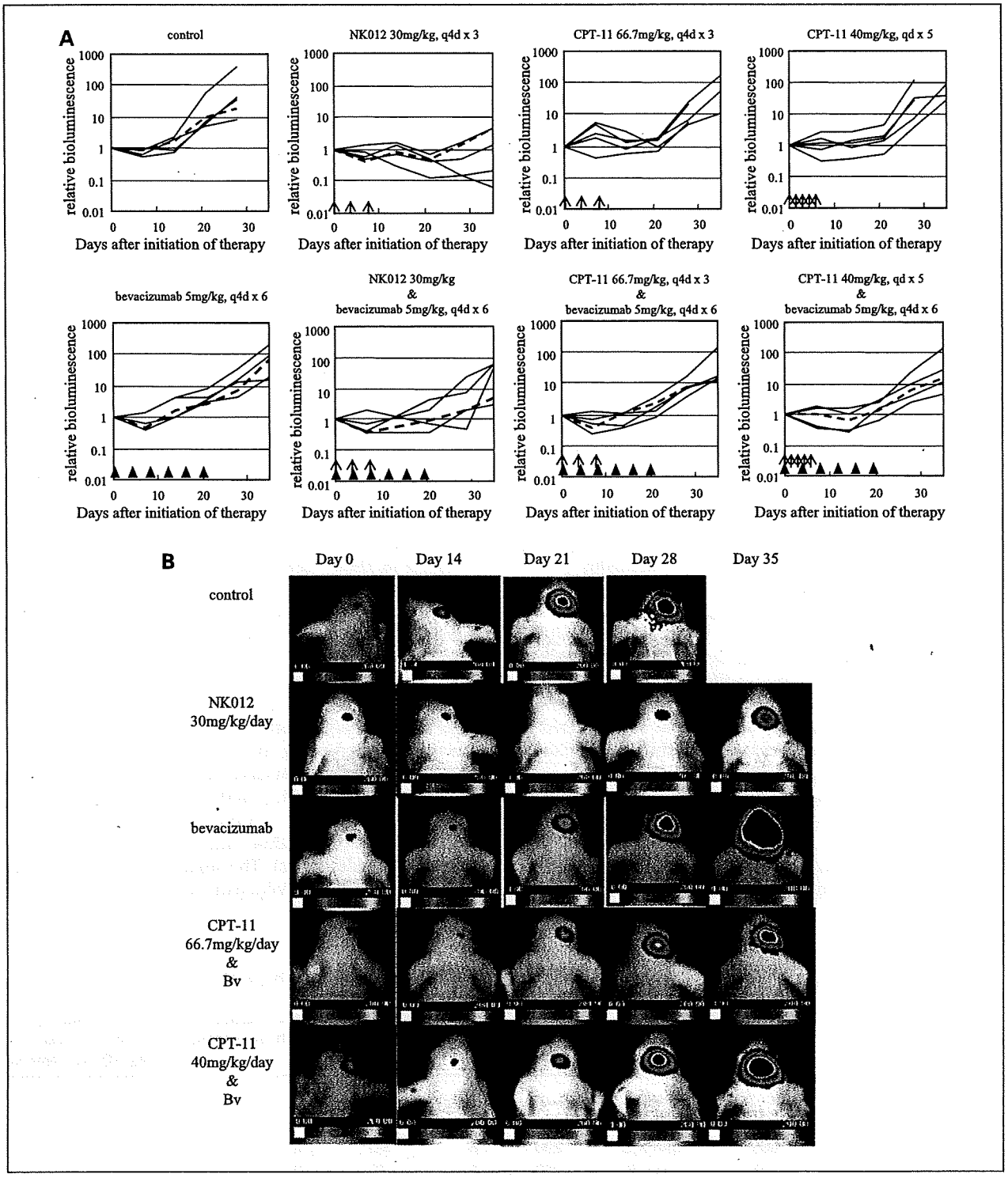

Fig. 1. Effects of NK012 and CPT-11 in U87MG/Luc mouse models. Cells were injected intracranially in athymic mice. Treatments were initiated 8 d after tumor inoculation with NK012, 30 mg/kg intravenously, thrice every 4 d; CPT-11, 67 mg/kg intravenously, thrice every 4 d; CPT-11, 40 mg/kg intravenously, daily over 5 consecutive d; bevacizumab, 5 mg/kg intraperitoneally, six times every 4 d; or both modalities and 0.9% NaCl solution control. ↑, NK012 or CPT-11 intravenous administration; ▲, bevacizumab intraperitoneal administration. *A*, antitumor activity of NK012 or CPT-11 was evaluated by counting the number of photons using the Photon Imager system. The discontinued lines in some of the graphs represent individuals that died during the experimental course and the subsequent assay was not conducted. The dashed lines correspond to the mice of each therapy expressed in *B*. *B*, images of U87MG/Luc mouse model treated with each regimen taken using the Photon Imager system on days 0, 14, 21, 28, and 35 after the initiation of therapy. Data derived from the same mice are expressed as dashed lines in *A*.

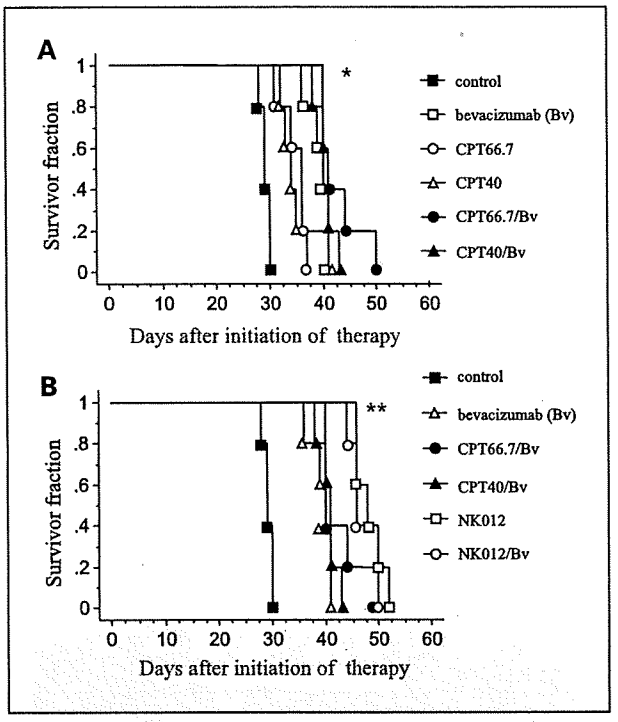

Fig. 2. Survival curves of U87MG/Luc mouse models in each regimen. *A*, ■, 0.9% NaCl solution; □, bevacizumab, 5 mg/kg, q4d × 6; ●, CPT-11, 66.7 mg/kg, q4d × 3 with bevacizumab, 5 mg/kg, q4d × 6; ▲, CPT-11, 40 mg/kg, qd × 5 with bevacizumab, 5 mg/kg, q4d × 6; O, CPT-11, 66.7 mg/kg, q4d × 3; Δ, CPT-11, 40 mg/kg, qd × 5. CPT-11/bevacizumab is significantly superior to CPT-11 monotherapy [CPT66.7 versus CPT66.7/bevacizumab ($P < 0.01$) and CPT40 versus CPT40/bevacizumab ($P < 0.05$)]. *B*, □, NK012, 30 mg/kg/d, q4d × 3; O, NK012, 30 mg/kg/d with bevacizumab, 5 mg/kg, q4d × 6; Δ, bevacizumab, 5 mg/kg, q4d × 6; ■, 0.9% NaCl solution; ●, CPT-11, 66.7 mg/kg, q4d × 3 with bevacizumab, 5 mg/kg, q4d × 6; ▲, CPT-11, 40 mg/kg, qd × 5 with bevacizumab, 5 mg/kg, q4d × 6. NK012 monotherapy is significantly superior to CPT66.7/bevacizumab ($P < 0.01$) and CPT40/bevacizumab ($P < 0.05$).

from the ileocecal junction for the ileum. Samples were fixed in 10 formalin, embedded in paraffin, sectioned, and stained with H&E. Inflammation was scored by using an inflammation scale from - to ++, with - indicating absent inflammation, + indicating mild inflammation predominantly infiltrated with lymphocytes, and ++ indicating active inflammation infiltrated with lymphocytes and neutrophils. All histopathologic and immunohistologic analysis and interpretation were done directly by an experienced pathologist.

Pharmacokinetics study of NK012 and CPT-11 combined with bevacizumab. Four mice bearing U87MG/Luc tumor per group were used for the biodistribution analysis of NK012 and CPT-11. Twenty-eight days after the intracranial injection of U87MG/Luc cells, NK012 (30 mg/kg) or CPT-11 (66.7 mg/kg) was intravenously administered with or without simultaneous intraperitoneal administration of bevacizumab (5 mg/kg) to the mice. After euthanasia, tumor tissues were obtained at T_{max} of each drug, 12 h after NK012 and 3 h after CPT-11 administration, respectively (12, 13). Each tumor was excised without the adjacent normal brain tissue. The size of tumor was ~5 mm in diameter. The tumor samples were rinsed with 0.9% NaCl solution, mixed with 0.1 mol/L glycine-HCl buffer (pH 3.0)/methanol at 5% (w/w), and then homogenized using Precellys 24 (Bertin Technologies). The samples were vortexed vigorously for 10 s and then filtered through an Ultrafree-MC centrifugal filter device with a cutoff molecular diameter of 0.45 μm (Millipore). We had confirmed that the filtered solution contained only free SN-38. Reverse-phase high-performance liquid chromatography was done at 35°C on a Mightysil RP-18 GP column 150 × 4.6 mm (Kanto Chemical). Fifty microliters of a sample were injected into an Alliance 2795 high-performance liquid chromatography system (Waters Associates) equipped with a Waters 2475 multi λ fluorescence detector. The mobile phase was a mixture of 100 nmol/L ammonium acetate (pH 4.2) and methanol (11:9, v/v). The flow rate was 1.0 mL/min. The content of SN-38 was calculated by measuring the relevant peak area for calibration against the corresponding peak area derived from the CPT internal standard. Peak data were recorded using a chromatography management system (MassLynx version 4.0; Waters Associates).

Statistical analysis. Data were expressed as mean ± SD. Significance of differences was calculated using the unpaired two-tailed *t* test with StatView 5.0. $P < 0.05$ was regarded as statistically significant. Kaplan-Meier analysis was done to determine the antitumor activity of each treatment on the time to morbidity, and statistical differences were ranked accordingto the Breslow-Gehan-Wilcoxon test using StatView 5.0. To evaluate the change in photon count of each treatment group, repeated-measures ANOVA was done.

Results

Antitumor response of U87MG xenograft. NK012 at the MTD (30 mg/kg/d) administered thrice every 4 days proved to be the most active against xenografts, with three tumor regressions and tumor growth delay of >18 days (Table 1). In combination with bevacizumab, CPT-11 at the MTD (66.7 mg/kg/d) administered thrice every 4 days and at the MTD (40 mg/kg/d) administered daily over 5 consecutive days induced two tumor regressions and tumor growth delay of 7 and 8 days, respectively. Without bevacizumab, CPT-11 at the MTD (40 mg/kg) administered daily over 5 consecutive days induced one tumor regression (Table 1). Comparison of the relative photon counts on repeated-measures ANOVA (days 0-28) revealed significant differences in photon counts between mice treated with NK012 and those treated with CPT-11 (66.7 mg/kg/d, q4d × 3) in combination with bevacizumab ($P = 0.02$; Fig. 1A and B). Tendency of differences between mice treated with NK012 and those treated with CPT-11 (40 mg/kg/d, qd × 5) in combination with bevacizumab ($P = 0.14$) was observed (Fig. 1A and B).

The median overall survival time was most prolonged in the NK012 (30 mg/kg/d, q4d × 3) group for 1 week

compared with the CPT-11/bevacizumab group (Table 1). The CPT-11 group with bevacizumab showed longer median overall survival time compared with the CPT-11 monotherapy group with two schedules: 66.7 mg/kg/d, q4d × 3, and 40 mg/kg/d, qd × 5, respectively (Table 1). Kaplan-Meier analysis showed a significant survival benefit of the CPT-11/bevacizumab group compared with the CPT-11 monotherapy (66.7 mg/kg/d, q4d × 3; P = 0.004) and CPT-11 (40 mg/kg/d, qd × 5; P = 0.036), respectively (Fig. 2A). Furthermore, Kaplan-Meier analysis showed a significant survival benefit in the NK012 group compared with the CPT-11 (66.7 mg/kg/d, q4d × 3)/bevacizumab group (P = 0.046) and CPT-11 (40 mg/kg/d, qd × 5)/bevacizumab group (P = 0.0041), respectively (Fig. 2B). However, there was no significant difference between NK012/bevacizumab group and NK012 monotherapy group (P = 0.45; Fig. 2B). There was no severe body weight loss or toxic death according to treatment (Table 1).

Histologic results. Histologic examinations revealed that decreased cellularity, increased tumor stroma, and inflammatory cell infiltration were observed in the tumors treated with NK012. Tumors treated with other regimens showed no apparent morphologic differences from the control tumors (Fig. 3A). Concordant with morphologic changes, the number of Ki-67$^+$ tumor cells decreased in tumors treated with NK012 compared with CPT-11/bevacizumab (Fig. 3A and B; $P < 0.001$). Quantification of VEGF-positive area and microvessel density decreased in tumors treated with NK012 compared with other treatment regimens (Fig. 3A, C, and D; $P < 0.05$). Microvessel density dramatically decreased in tumors treated with bevacizumab in combination with any formulation of the anticancer drug (Fig. 3A and C). The small intestinal mucosa of mice treated

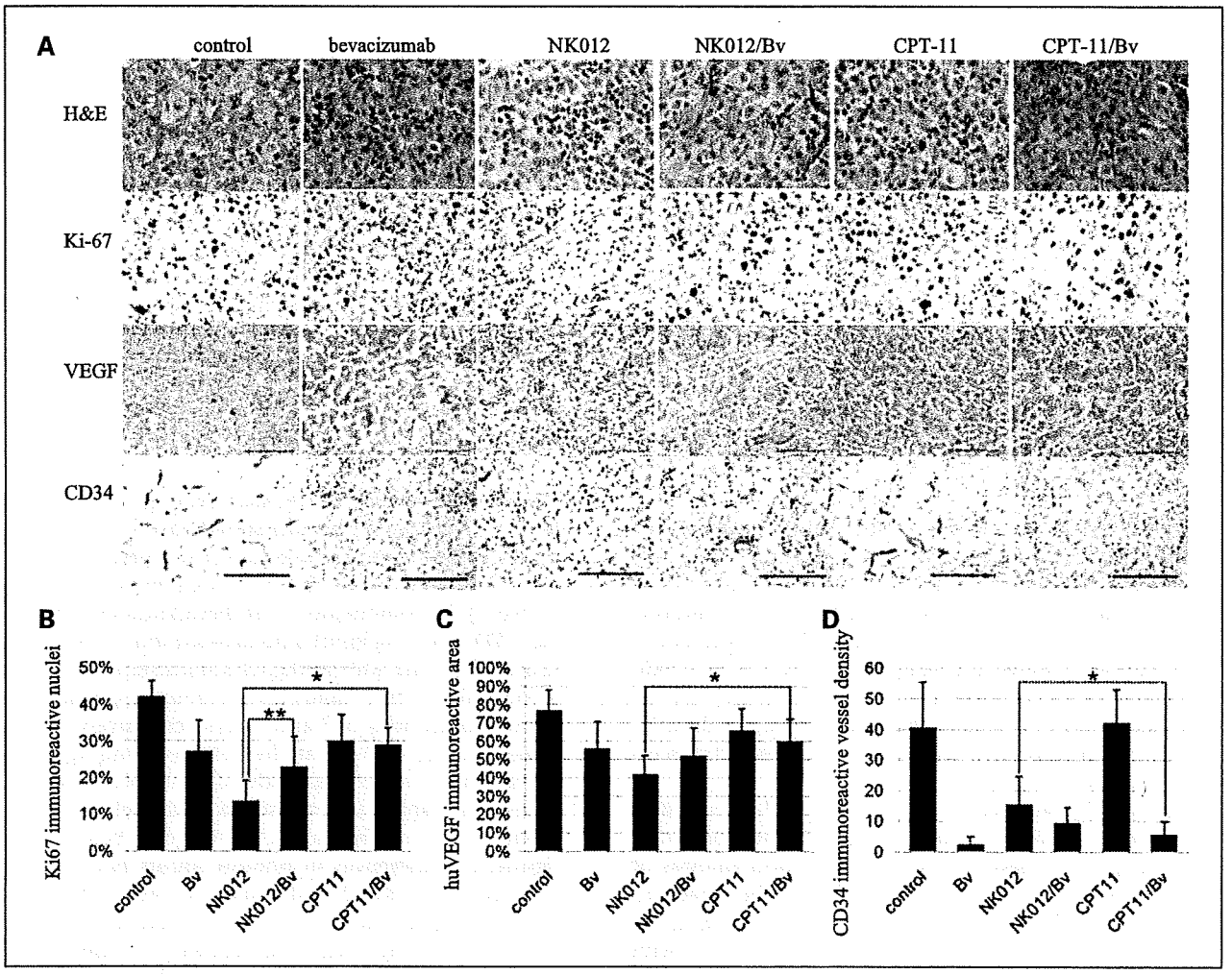

Fig. 3. Tissue-based studies of U87MG/Luc orthotopic xenografts of nude mice treated with NK012, CPT-11, bevacizumab, NK012/bevacizumab, or CPT-11/bevacizumab. *A*, H&E staining of representative xenograft regions (magnification, ×400). Immunohistochemical analysis of tumor cells stained with anti–Ki-67 nuclear antigen, anti-VEGF, and angiogenesis with anti-CD34 antibody (bar, 100 μm). Comparison between xenografts treated with each regimen. *B*, proliferation index by Ki-67. *C*, human VEGF immunoreactive area (%). *D*, angiogenesis by vessel density. *, $P < 0.01$; **, $P < 0.05$ (two-tailed Student's t test).

with NK012 or NK012/bevacizumab showed no histologic changes including fibrosis, active inflammation, or shortening and decrease in number of villi in the small intestinal mucosa as reported previously (ref. 17; data not shown).

Tissue concentration of free SN-38 after administration of NK012 and CPT-11 in combination with bevacizumab. The concentration of free SN-38 in orthotopic glioblastoma tissue after the administration of NK012 and CPT-11 in combination with bevacizumab was examined to evaluate the interaction between these anticancer agents. In the case of NK012 administration in combination with bevacizumab, free SN-38 concentration in tumor tissue was significantly decreased compared with SN-38 concentration when NK012 was administered alone (Fig. 4A; $P = 0.027$). On the other hand, in the case of CPT-11 administration in combination with bevacizumab, free SN-38 concentration in tumor tissue was almost similar to SN-38 concentration when CPT-11 was administered alone (Fig. 4B; $P = 0.66$).

Discussion

Concomitant chemoradiotherapy with surgery followed by single-agent adjuvant treatment with the alkylating agent temozolomide is the current standard of care for the patients with glioblastoma multiforme (3). However, tumor recurrence is experienced by almost all glioblastoma multiforme patients after the first-line therapy. Combination therapy of CPT-11 with bevacizumab is now a recognized second-line therapy in recurrent glioblastoma multiforme.

The main purpose of this study was to clarify the advantage of combination therapy of NK012, a SN-38–incorporating polymeric micelle, with bevacizumab against orthotopic U87MG glioblastoma multiforme tumor in mice. Single use of NK012 exerted superior antitumor activity in the orthotopic tumors compared with CPT-11 combined with bevacizumab. The NK012 single-agent treatment group showed the most prolonged survival of all treatment groups, and a statistically significant difference was revealed by the Kaplan-Meier analysis compared with the CPT-11/bevacizumab group (66.7 mg/kg/d, q4d × 3; $P = 0.046$ and 40 mg/kg/d, qd × 5; $P = 0.0041$).

The present study showed that the addition of the anti-VEGF monoclonal antibody bevacizumab to the CPT-11 therapy resulted in markedly increased activity, the same as reported clinically (9, 10). Although the mechanisms underlying the activities of bevacizumab remain unclear, the following factors are considered to be important: direct antiangiogenic effects and cytotoxics against vascular endothelial cells and other stromal elements, direct effects on tumor cells expressing VEGF receptors and stem cell–like glioma cells (18), and improvement of the delivery of anticancer drug by forced normalization of tumor vasculature (19). Bevacizumab is a humanized monoclonal antibody that does not cross-react with mouse VEGF, and the efficacy and toxicity in combination with cytotoxic drugs are not the same in mouse and human. In mice, however, bevacizumab can react with VEGF secreted from human tumor xenograft and leads to tumor vessel decrease, reduction in vessel permeability and diameter (20), and decrease in interstitial fluid pressure in xenografts (21).

NK012, a novel SN-38–incorporating polymeric micelle, is a prodrug of SN-38 similar to CPT-11. Although CPT-11 is converted to SN-38 in tumors by carboxylesterase, the metabolic conversion rate is within 2% to 8% of the original volume of CPT-11 (22, 23). In contrast, the release rate of SN-38 from NK012 is 74% under physiologic pH conditions even without carboxylesterases (12). Recently, we showed that NK012 exerted significantly more potent antitumor activity against various human tumor xenografts compared with CPT-11 (12, 24–26). The diameter of a micelle carrier is in the approximate range of 10 to 100 nm. Although this size is small, it is still sufficiently large to prevent renal secretion of the carrier. The micelle system can evade nonspecific capture by the

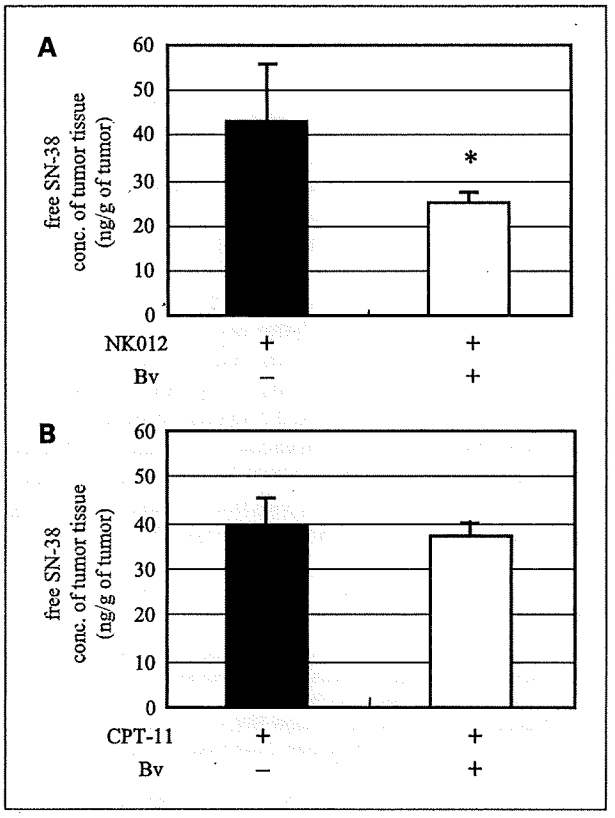

Fig. 4. Concentration of free SN-38 of tumor tissue at T_{max}. NK012 (30 mg/kg intravenously), CPT-11 (66.7 mg/kg intravenously), or bevacizumab (5 mg/kg intraperitoneally) was administered 28 d after intracranial injection of U87MG/Luc (*columns*, mean; *bars*, SD). *A*, concentration (*conc.*) of free SN-38 in glioma tissue of U87MG/Luc mouse model after administration of NK012 alone (*black column*) and NK012 with bevacizumab (*white column*). *B*, concentration of free SN-38 in glioma tissue of U87MG/Luc mouse model after administration of CPT-11 alone (*black column*) and CPT-11 with bevacizumab (*white column*). *, $P < 0.05$, significant to NK012 alone (two-tailed Student's *t* test).

reticuloendothelial system in various organs because the outer shell of the micelle is covered with polyethylene glycol. Therefore, a drug-incorporating micelle can be expected to have a long plasma half-life, which permits a large amount of the micelles to reach tumor tissues, extravasate from tumor capillaries, and then be retained in tumor tissues for a long time by using the enhanced permeability and retention effect (11). This prolonged retention of NK012 in the tumor and sustained release of free SN-38 from NK012 may be responsible for its more potent antitumor activity observed in the present study (27).

In this study, the antitumor effect was observed by means of bioluminescence imaging. Bioluminescence imaging revealed antitumor activity compared with CPT-11 in combination with bevacizumab. However, antiangiogenic agents can suppress the extravasation of contrast agents such as gadolinium, and gadolinium-contrast magnetic resonance imaging may give a false response (28). This means that bevacizumab is suspected of having a negative effect on bioluminescence imaging by reducing the permeability of tumor vessels. Therefore, we also evaluated the antitumor activity pathologically and immunohistochemically. Consequently, the NK012 group showed a high therapeutic advantage in Ki-67 index in a pathology analysis compared with the other treatment groups.

Interestingly, bevacizumab could not potentiate the antitumor activity of NK012 and elongate the survival of NK012. In the present pharmacologic study, the free SN-38 concentration in the tumor tissue decreased significantly when NK012 was administered in combination with bevacizumab compared with NK012 monotherapy. Results available to date and the results from the present study lead to the consideration that the reduced accumulation of NK012 by bevacizumab may cancel the direct effect of bevacizumab and NK012 against orthotopic glioma in mice. The influence of bevacizumab might be different in macromolecule such as NK012 and small compound such as CPT-11. Enhanced vascular permeability might be more important for macromolecule than small molecule. A further study is necessary to clarify the phenomenon. Dose-limiting toxicities of CPT-11 are neutropenia and diarrhea. Diarrhea was not observed in the NK012 treatment group, and the intestinal toxicity was not observed by the pathology examination as reported previously (17). As for this, it is understood that serious diarrhea has not been reported in MTD of NK012 in two phase I clinical trials against advanced solid tumors in Japan and the United States (29, 30).

In conclusion, NK012 showed a higher therapeutic index in U87MG glioblastoma in mice compared with CPT-11/bevacizumab. Therefore, data from the present study may warrant further preclinical evaluation of NK012 before conducting the clinical trial of the drug.

Disclosure of Potential Conflicts of Interest

No potential conflicts of interest were disclosed.

Acknowledgments

We thank N. Mie and M. Ohtsu for technical assistance and K. Shiina for secretarial assistance.

Grant Support

Grant-in-Aid for Third-Term Comprehensive Control Research for Cancer from the Ministry of Health, Labor and Welfare of Japan; grant 17016087 for Scientific Research on Priority Areas from the Ministry of Education, Culture, Sports, Science and Technology; and Japanese Foundation for Multidisciplinary Treatment of Cancer (Y. Matsumura) and Princess Takamatsu Cancer Research Fund 07-23908.

The costs of publication of this article were defrayed in part by the payment of page charges. This article must therefore be hereby marked *advertisement* in accordance with 18 U.S.C. Section 1734 solely to indicate this fact.

Received 9/2/09; revised 11/2/09; accepted 11/9/09; published OnlineFirst 1/12/10.

References

1. Takano S, Yoshii Y, Kondo S, et al. Concentration of vascular endothelial growth factor in the serum and tumor tissue of brain tumor patients. Cancer Res 1996;56:2185–90.
2. Kleihues P, Louis DN, Scheithauer BW, et al. The WHO classification of tumors of the nervous system. J Neuropathol Exp Neurol 2002;61:215–25, discussion 226–9.
3. Stupp R, Mason WP, van den Bent MJ, et al. Radiotherapy plus concomitant and adjuvant temozolomide for glioblastoma. N Engl J Med 2005;352:987–96.
4. Wong ET, Hess KR, Gleason MJ, et al. Outcomes and prognostic factors in recurrent glioma patients enrolled onto phase II clinical trials. J Clin Oncol 1999;17:2572–8.
5. Friedman HS, Petros WP, Friedman AH, et al. Irinotecan therapy in adults with recurrent or progressive malignant glioma. J Clin Oncol 1999;17:1516–25.
6. Cloughesy TF, Filka E, Kuhn J, et al. Two studies evaluating irinotecan treatment for recurrent malignant glioma using an every-3-week regimen. Cancer 2003;97:2381–6.
7. Chamberlain MC. Salvage chemotherapy with CPT-11 for recurrent glioblastoma multiforme. J Neurooncol 2002;56:183–8.
8. Prados MD, Lamborn K, Yung WK, et al. A phase 2 trial of irinotecan (CPT-11) in patients with recurrent malignant glioma: a North American Brain Tumor Consortium study. Neuro Oncol 2006;8:189–93.
9. Vredenburgh JJ, Desjardins A, Herndon JE 2nd, et al. Phase II trial of bevacizumab and irinotecan in recurrent malignant glioma. Clin Cancer Res 2007;13:1253–9.
10. Vredenburgh JJ, Desjardins A, Herndon JE 2nd, et al. Bevacizumab plus irinotecan in recurrent glioblastoma multiforme. J Clin Oncol 2007;25:4722–9.
11. Matsumura Y, Maeda H. A new concept for macromolecular therapeutics in cancer chemotherapy: mechanism of tumoritropic accumulation of proteins and the antitumor agent smancs. Cancer Res 1986;46:6387–92.
12. Koizumi F, Kitagawa M, Negishi T, et al. Novel SN-38-incorporating polymeric micelles, NK012, eradicate vascular endothelial growth factor-secreting bulky tumors. Cancer Res 2006;66:10048–56.

13. Kuroda J, Kuratsu J, Yasunaga M, Koga Y, Saito Y, Matsumura Y. Potent antitumor effect of SN-38-incorporating polymeric micelle, NK012, against malignant glioma. Int J Cancer 2009;124: 2505–11.
14. Vassal G, Terrier-Lacombe MJ, Bissery MC, et al. Therapeutic activity of CPT-11, a DNA-topoisomerase I inhibitor, against peripheral primitive neuroectodermal tumour and neuroblastoma xenografts. Br J Cancer 1996;74:537–45.
15. Kawato Y, Furuta T, Aonuma M, Yasuoka M, Yokokura T, Matsumoto K. Antitumor activity of a camptothecin derivative, CPT-11, against human tumor xenografts in nude mice. Cancer Chemother Pharmacol 1991;28:192–8.
16. Vassal G, Boland I, Santos A, et al. Potent therapeutic activity of irinotecan (CPT-11) and its schedule dependency in medulloblastoma xenografts in nude mice. Int J Cancer 1997;73:156–63.
17. Nagano T, Yasunaga M, Goto K, et al. Antitumor activity of NK012 combined with cisplatin against small cell lung cancer and intestinal mucosal changes in tumor-bearing mouse after treatment. Clin Cancer Res 2009;15:4348–55.
18. Bao S, Wu Q, Sathornsumetee S, et al. Stem cell-like glioma cells promote tumor angiogenesis through vascular endothelial growth factor. Cancer Res 2006;66:7843–8.
19. Weis SM, Cheresh DA. Pathophysiological consequences of VEGF-induced vascular permeability. Nature 2005;437:497–504.
20. Yuan F, Chen Y, Dellian M, Safabakhsh N, Ferrara N, Jain RK. Time-dependent vascular regression and permeability changes in established human tumor xenografts induced by an anti-vascular endothelial growth factor/vascular permeability factor antibody. Proc Natl Acad Sci U S A 1996;93:14765–70.
21. Lee CG, Heijn M, di Tomaso E, et al. Anti-vascular endothelial growth factor treatment augments tumor radiation response under normoxic or hypoxic conditions. Cancer Res 2000;60:5565–70.
22. Slatter JG, Schaaf LJ, Sams JP, et al. Pharmacokinetics, metabolism, and excretion of irinotecan (CPT-11) following I.V. infusion of [(14)C] CPT-11 in cancer patients. Drug Metab Dispos 2000;28:423–33.
23. Rothenberg ML, Kuhn JG, Burris HA 3rd, et al. Phase I and pharmacokinetic trial of weekly CPT-11. J Clin Oncol 1993;11:2194–204.
24. Sumitomo M, Koizumi F, Asano T, et al. Novel SN-38-incorporated polymeric micelle, NK012, strongly suppresses renal cancer progression. Cancer Res 2008;68:1631–5.
25. Nakajima TE, Yasunaga M, Kano Y, et al. Synergistic antitumor activity of the novel SN-38-incorporating polymeric micelles, NK012, combined with 5-fluorouracil in a mouse model of colorectal cancer, as compared with that of irinotecan plus 5-fluorouracil. Int J Cancer 2008;122:2148–53.
26. Saito Y, Yasunaga M, Kuroda J, Koga Y, Matsumura Y. Enhanced distribution of NK012, a polymeric micelle-encapsulated SN-38, and sustained release of SN-38 within tumors can beat a hypovascular tumor. Cancer Sci 2008;99:1258–64.
27. Kawato Y, Aonuma M, Hirota Y, Kuga H, Sato K. Intracellular roles of SN-38, a metabolite of the camptothecin derivative CPT-11, in the antitumor effect of CPT-11. Cancer Res 1991;51:4187–91.
28. Olivero WC, Dulebohn SC, Lister JR. The use of PET in evaluating patients with primary brain tumours: is it useful? J Neurol Neurosurg Psychiatry 1995;58:250–2.
29. Burris HA 3rd, Infante JR, Spigel DR, et al. A phase I dose-escalation study of NK012. Proc Am Soc Clin Oncol 2008, abstract 2538.
30. Kato K, Hamaguchi T, Shirao K, et al. Interim analysis of phase I study of NK012, polymer micelle SN-38, in patients with advanced cancer. Proc Am Soc Clin Oncol 2008, abstract 485.

EUROPEAN JOURNAL OF CANCER XXX (2009) XXX–XXX

available at www.sciencedirect.com

ScienceDirect

journal homepage: www.ejconline.com

Antitumour activity of NK012, SN-38-incorporating polymeric micelles, in hypovascular orthotopic pancreatic tumour

Yohei Saito [a,b], *Masahiro Yasunaga* [a], *Jun-ichiro Kuroda* [a], *Yoshikatsu Koga* [a], *Yasuhiro Matsumura* [a,*]

[a] *Investigative Treatment Division, Research Center for Innovative Oncology, National Cancer Center Hospital East, 6-5-1 Kashiwanoha, Kashiwa, Chiba 277-8577, Japan*

[b] *Laboratory of Cancer Biology, Department of Integrated Biosciences, Graduate School of Frontier Sciences, The University of Tokyo, 5-1-5 Kashiwanoha, Kashiwa, Chiba 277-8562, Japan*

ARTICLE INFO

Article history:
Received 10 September 2009
Received in revised form 6 November 2009
Accepted 19 November 2009
Available online xxxx

Keywords:
Pancreatic cancer
DDS (drug delivery system)
Polymer micelles
NK012

ABSTRACT

Human pancreatic cancer is refractory to chemotherapy partly because of blockage to penetration of anticancer agents. This issue must be taken into account particularly for the drug delivery system (DDS). The aim of the present study is to investigate how NK012 (SN-38-incorporating polymeric micelles) categorised as DDS exerts its antitumour effect in an orthotopic pancreatic tumour model compared with gemcitabine and irinotecan hydrochloride (CPT-11), a low-molecular-weight prodrug of a 7-ethyl-10-hydroxy-camptothecin (SN-38).

The maximum tolerated doses (MTDs) of NK012 (30 mg/kg/d), CPT-11 (66.7 mg/kg/d) and gemcitabine (16.5 mg/kg/d) were administered to mice bearing human pancreatic cancer cell (SUIT-2) xenografts implanted orthotopically. Antitumour effects of these compounds were evaluated. Drug distribution within the tumour was examined by fluorescence microscopy and high performance liquid chromatography (HPLC).

NK012 exerted potent antitumour effects compared with CPT-11 and gemcitabine. A high concentration of NK012 and SN-38 released from NK012 had been observed until 192 h. On the other hand, SN-38 converted from CPT-11 was detected only 1 h postinjection. Fluorescence from NK012 was detected up to 48 h, whereas that from CPT-11 almost disappeared by 24 h postinjection.

NK012 appeared to exert potent antitumour activity against intractable stroma-rich orthotopic pancreatic tumour xenografts due to its sufficient accumulation followed by the effective sustained release of SN-38 from NK012.

1. Introduction

Human pancreatic cancer is well known to have the worst prognosis.[1] At the time of diagnosis, the vast majority of the cancer extends beyond the pancreas. Direct invasion to nearby organs such as the stomach, duodenum, colon, spleen and kidney is common. Distant metastasis to the liver and peritoneal dissemination are also common.[2,3] Gemcitabine is a first-line therapy for patients with advanced pancreatic cancer; however, only a response rate within 6–11% was observed in pancreatic cancer patients treated with gemcitabine.[4,5] The recent success of molecular-targeting agents has some

* *Corresponding author:* Tel./fax: +81 4 7134 6857.
E-mail address: yhmatsum@east.ncc.go.jp (Y. Matsumura).

0959-8049/$ - see front matter
doi:10.1016/j.ejca.2009.11.014

Please cite this article in press as: Saito Y et al., Antitumour activity of NK012, SN-38-incorporating polymeric micelles, in hypovascular orthotopic pancreatic tumour, *Eur J Cancer* (2009), doi:10.1016/j.ejca.2009.11.014

impact on pancreatic cancer treatment. A recent phase III trial of gemcitabine alone versus gemcitabine and erlotinib (a tyrosine kinase inhibitor) in patients with advanced pancreatic cancer showed that overall survival was significantly improved with gemcitabine and erlotinib than with gemcitabine and placebo. However, the improvement in median overall survival with gemcitabine and erlotinib was modest (6.24 months versus 5.91 months).[6] Therefore, novel therapeutic approaches against invasive advanced pancreatic cancer are urgently needed.

There are several reasons why pancreatic cancer is intractable clinically. One is that anticancer drugs are not efficiently and sufficiently delivered to the cancer cells within pancreatic cancer tissues. This is because human pancreatic cancer is hypovascular[7,8] and is rich in interstitial tissue, which may hinder the efficient distribution of anticancer drugs to the entire pancreatic cancer tissue.

Passive targeting by the drug delivery system is based on the pathological features of many kinds of solid tumours. Solid tumours generally have the features of hypervascularity, irregular vascular architecture, enhanced vascular permeability and the absence of an effective lymphatic drainage that prevents efficient clearance of macromolecules. Using these characteristic tumour vasculatures, macro-molecular agents accumulate selectively in solid tumours compared with low-molecular agents, with less distribution to normal tissues. These vascular characteristics of solid tumours are the basis of the enhanced permeability and retention (EPR) effect.[9]

SN-38, a biologically active metabolite of CPT-11 has potent antitumour activity against several cancers.[10,11] However, it has not yet been used clinically because of its water insolubility and severe toxicity.[12,13] It has been recently shown that NK012, SN-38-incorporating polymeric micelles, can accumulate selectively in solid tumours by utilising the EPR effect and exerts significantly more potent activity against various human tumour xenografts than CPT-11.[14–18] In pancreatic cancer, we found that NK012 but not CPT-11 could eradicate subcutaneous pancreatic tumour xenografts[19] because of enhanced accumulation, distribution and retention within tumour tissues and the sustained release of SN-38 from NK012.

In the present study, we examined the antitumour effects and pharmaceutical features of NK012 compared with those of CPT-11 and gemcitabine using orthotopic human pancreatic cancer xenografts that are more similar to human pancreatic cancers in terms of tumour vascularity and interstitium.

2. Materials and methods

2.1. *Drugs and cells*

NK012 was prepared and supplied by Nippon Kayaku Co., Ltd. (Tokyo, Japan). CPT-11 was purchased from Yakult Co., Ltd. (Tokyo, Japan). SN-38 was supplied by Yakult Co., Ltd. Gemcitabine was purchased from Eli Lilly Japan K.K. (Kobe, Japan). The human pancreatic cancer cell line SUIT-2 was purchased from the Health Science Research Resources Bank (Osaka, Japan). SUIT-2 cells were maintained in Dulbecco's modified Eagle's medium supplemented with 10% foetal bovine serum (Cell Culture Technologies, Gaggenau-Hoerden, Germany), 100 units/ml streptomycin and 2 mmol/L L-glutamine (Sigma, St. Louis, MO, United States of America) in an atmosphere of 5% CO_2 at 37 °C.

2.2. *Orthotopic pancreatic cancer mouse model*

Four-weeks-old female BALB/c nude mice were purchased from CLEA Japan (Tokyo, Japan). SUIT-2 cells (5×10^6) were injected into the body of the pancreas of nude mouse after laparotomy under anaesthesia. All animal procedures were performed in compliance with the Guideline for the Care and Use of Experimental Animals established by the Committee for Animal Experimentation of the National Cancer Center, Japan; these guidelines meet the ethical standards required by law for the use of experimental animals in Japan.

2.3. *In vitro growth inhibition assay*

Cell toxicity of NK012, SN-38, CPT-11 and gemcitabine was measured by tetrazolium salt-based proliferation assay (WST-8 assay; Wako Chemicals, Osaka, Japan), as described previously.[19] Data were averaged and normalised against a non-treated control to generate dose–response curves. The number of living cells (% Control) was calculated using the following formula: % Control = (Each absorbance – Absorbance of blank well)/Absorbance of control well × 100.

2.4. *Establishment of SUIT-2 cell lines stably expressing firefly luciferase and YFP mutant Venus*

For the *in vivo* bioluminescence imaging of orthotopic pancreatic tumours, the SUIT-2 cell line stably expressing firefly luciferase and the yellow fluorescent protein (YFP) mutant Venus were established. The coding sequence for firefly luciferase and Venus was subcloned into the pIRES Vector (Clontech Laboratories, Mountain View, CA, United States of America). The fragment consists of Luciferase-IRES-Venus generated from the plasmid with the restriction enzymes Nhe I and Not I. This fragment was subcloned into the pEF6/V5-His Vector (Invitrogen, Carlsbad, CA, United States of America) to generate plasmids of pEF6-Luciferase-IRES-Venus. SUIT-2 cells were transfected with these plasmids. Thereafter, we established SUIT-2 cell lines stably expressing firefly luciferase and the YFP mutant Venus.

2.5. *Histological and immunohistochemical analyses*

Tumour tissues were fixed in 10% formalin, and paraffin sections were prepared by the Tokyo Histopathologic Laboratory Co., Ltd. (Tokyo, Japan). For blood vessel staining, the sections were soaked 3 times for 5 min each in xylene, and then 3 times for 3 min each in ethanol to remove the paraffin. The sections were then rinsed with phosphate buffered saline (PBS), and endogeneous peroxidase was blocked with a 0.3% hydrogen peroxide solution in 100% methanol for 20 min, followed by 3 times of PBS rinses for 5 min. Then, Proteinase K (Dako, Glostrup, Denmark) was added. After the sections were rinsed 3 times for 5 min each with PBS, non-specific protein binding was blocked with 5% skim milk (BD, Franklin Lakes, NJ, United States of America) in PBS for 30 min at room

Please cite this article in press as: Saito Y et al., Antitumour activity of NK012, SN-38-incorporating polymeric micelles, in hypovascular orthotopic pancreatic tumour, *Eur J Cancer* (2009), doi:10.1016/j.ejca.2009.11.014

temperature. After 3 times of PBS rinses for 5 min, a polyclonal antibody against factor VIII (Invitrogen) was added at a dilution of 1:50, followed by incubation for 1 h and 3 times of PBS rinses for 5 min each. Biotinylated anti-rabbit IgG was added at a dilution of 1:50, followed by incubation for 1 h. The sections were rinsed 3 times with PBS, and Vectastain Elite ABC Reagent (Vector Laboratories, Burlingame, CA, United States of America) was used. The sections were rinsed again 3 times with PBS and incubated with 3,3′-diaminobenzidine tetrahydrochloride (DAB+) Liquid System (Dako) for 30 s. Finally, the sections were rinsed and counterstained with haematoxylin solution.

2.6. *In vivo growth inhibition assay*

2.6.1. *Experiment 1*

Orthotopic mice bearing a pancreatic tumour were randomly divided into four groups consisting of five mice per group. The maximum tolerated doses (MTDs) of NK012 (30 mg/kg at SN-38 equivalents dose, 0.076 mmol/kg) and CPT-11 (66.7 mg/kg; 0.098 mmol/kg) were intravenously injected on days 0 (21 d after tumour inoculation), 4 and 8. The MTD of gemcitabine (16.5 mg/kg) was administrated intraperitoneally on days 0, 3, 6 and 9 as described previously.[20] As a control, normal 0.9% NaCl solution was intravenously administered on days 0, 4 and 8. Kaplan–Meier analysis was performed to determine the effects of the drugs. Statistical differences were ranked according to the Mantel–Cox log-rank test using StatView 5.0. The percentage of Increase in Life Span (ILS%) was calculated as follows[21]: ILS% = $(T/C - 1) \times 100$. T is the median survival days in drug treatment mouse group and C is the median survival days in control mouse group.

2.6.2. *Experiment 2*

To assess the antitumour effects of NK012, CPT-11 and gemcitabine, *in vivo* bioluminescence imaging studies were performed using the Photon Imager animal imaging system (Biospace, Paris, France). For imaging, mice bearing orthotopic pancreatic tumour were simultaneously anesthetised with isoflurane and D-luciferine potassium salt (Synchem, Germany), normal 0.9% NaCl solution was intraperitoneally administrated at 125 mg/kg, and images were taken 5 min postinjection. For bioluminescence image analysis, regions of interest encompassing the area of a signal were defined using Photo Vision software (Biospace), and total numbers of photons per minute (cpm) were recorded. The pseudo-colour luminescent image from violet (least intense) to red (most intense) represented the spatial distribution of detected photon counts emerging from active luciferase within an animal. Twenty-one days after SUIT-2/Luc inoculation, treatment was conducted as described in Experiment 1. *In vivo* bioluminescence imaging studies were performed on days 0, 3, 6, 9 and 12 from the day of treatment initiation. To determine the effects of treatment on the time to change luminescence intensity, ANOVA analysis was carried out using StatView 5.0 software. $P < 0.05$ was considered significant.

2.6.3. *Experiment 3*

Mice bearing orthotopic pancreatic tumour were treated as described in Experiment 1. Twelve days later from treatment initiation, tumours were excised from the pancreas. Thereafter, the length (a) and width (b) of tumour masses were measured; tumour volume was calculated as follows: tumour volume = $(a \times b^2) \times 0.5233$. At the same time, we measured tumour weight.

To evaluate the metastatic nodules of the implanted pancreatic cancer, we measured nodule area in the mesentery.

2.7. *Evaluation of NK012 and CPT-11 distribution in tumour tissue by fluorescence microscopy*

The SUIT-2 orthotopic pancreatic tumour tissues described above were used for the analysis of the biodistributions of NK012 and CPT-11. Twenty-one days after the SUIT-2 cell inoculation, the MTD of NK012 (30 mg/kg) or CPT-11 (66.7 mg/kg) was injected intravenously into the tail vein of mice. 1, 6, 24 and 48 h after NK012 or CPT-11 injection, the mice were administered with fluorescein *Lycopersicon esculentum* lectin (100 μl/mouse) (Vector Laboratories) to visualise tumour blood vessels. After sacrificing the mice under anaesthesia, tumours were then excised and embedded in an optimal cutting temperature compound and were frozen at −80 °C until use. Tissue sections (6 μm thick) were prepared using Tissue-Tek Cryo3 (Sakura Finetek United States of America, Inc., Torrance, CA, United States of America), and the frozen sections were examined under a fluorescence microscope, BIOREVO BZ9000 (Keyence, Osaka, Japan), at an excitation wavelength of 377 nm and an emission wavelength 447 nm to evaluate the distributions of NK012 and CPT-11 within the tumour tissues. Because formulations containing SN-38 bound via ester bonds possess a particular fluorescence, both NK012 and CPT-11 could be detected under the same fluorescence conditions.

2.8. *Pharmacokinetics study of NK012 and CPT-11*

Mice bearing orthotopic SUIT-2 cells were used for the analysis of the biodistributions of NK012 and CPT-11. NK012 (30 mg/kg) and CPT-11 (66.7 mg/kg) were intravenously administered to mice bearing SUIT-2 cells or to normal mice. Mice were sacrificed under anaesthesia, and tumour and normal pancreatic tissues were obtained 1, 6, 24, 48, 72, 96, 120, 144, 168 and 192 h after NK012 or CPT-11 injection. Pharmacokinetics study was conducted as described previously.[14] Briefly, the tumour and normal pancreatic tissues were rinsed with physiological 0.9% NaCl solution, mixed with 0.1 M glycine–HCl buffer (pH 3.0)/methanol at w/w% and then homogenised. To analyse the concentration of free SN-38 and CPT-11, 100 μl of the tumour homogenates was mixed with 20 μl of 1 mM phosphoric acid/methanol (1:1), 40 μl of ultrapure water and 60 μl of camptothecin solution (10 ng/ml for SN-38 and 15 ng/ml for CPT-11) as an internal standard. The samples were vortexed vigorously for 10 s, and then filtered through Ultrafree-MC Centrifugal Filter Devices with a cut-off molecular diameter of 0.45 μm (Millipore Co., Bedford, MA, United States of America). Reversed-phase HPLC was performed at 35 °C on a Mightysil RP-18 GP column (150 × 4.6 mm; Kanto Chemical Co., Inc., Tokyo, Japan). A sample (50 μl) was injected into an Alliance Waters 2795 HPLC system (Waters, Milford, MA, United States of America) equipped

Please cite this article in press as: Saito Y et al., Antitumour activity of NK012, SN-38-incorporating polymeric micelles, in hypovascular orthotopic pancreatic tumour, *Eur J Cancer* (2009), doi:10.1016/j.ejca.2009.11.014

with a Waters 2475 multi λ fluorescence detector. Fluorescence originating from SN-38 was detected at 540 nm with an excitation wavelength of 365 nm and that originating from CPT-11 was detected at 430 nm with an excitation wavelength of 365 nm. The mobile phase was a mixture of 100 nmol/L ammonium acetate (pH 4.2) and methanol (11:9(v/v)). The flow rate was 1.0 ml/min. SN-38 content was calculated by measuring the relevant peak area and calibrating against the corresponding peak area derived from the CPT-11 internal standard. Peak area was recorded using a chromatography management system (MassLynx v4.0, Waters). In these experiments, limit of the detection of CPT-11 or SN-38 was 0.002 μg/g tumour or0.018 μg /g tumour, respectively.

For polymer-bound SN-38 detection, SN-38 was released from the conjugate. Briefly, 100 μl of tissue samples was diluted with 20 μl of methanol (50 w/w%) and 20 μl of NaOH (0.7 mol/L). The samples were incubated for 15 min at 25 °C. After incubation, 20 μl of HCl (0.7 mol/L) and CPT solution (10 ng/ml for SN-38 and 15 ng/ml for CPT-11) were added to the samples, and then the hydrolysate was filtered through a MultiScreen Solvinert. The filtrate (15 μl) was applied to the same HPLC system described above.

2.9. *Statistical analysis*

Student's t-test was used for the statistical analyses unless otherwise mentioned. $P < 0.05$ was considered significant.

3. Results

3.1. *In vitro cellular sensitivity of SUIT-2 cells to NK012, gemcitabine, CPT-11 and SN-38*

The inhibitory concentration 50% (IC_{50}) values showed that the growth inhibitory effects of NK012 were 100-fold more potent than those of CPT-11 against SUIT-2 cells. On the other hand, the IC_{50} values of NK012 were almost similar to those of SN-38 and gemcitabine (Fig. 1).

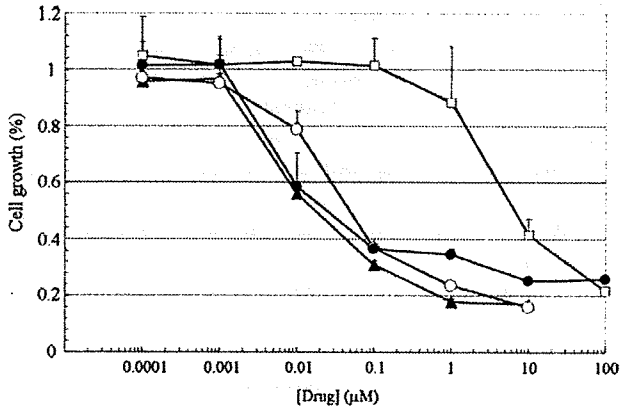

Fig. 1 – *In vitro* growth inhibitory activities of NK012, SN-38, CPT-11 and gemcitabin. Cell growth inhibitory activities of NK012, SN-38, CPT-11 and gemcitabin were measured using the WST-8 assay. SUIT-2 cells (5000 cells/well) in 96-well plates were incubated overnight. Growth medium was changed to new medium with various concentrations of NK012 (○), SN-38 (▲), CPT-11 (□) and gemcitabin (●). Cell viability was measured as described in Section . Points, mean; Bars, SD.

3.2. *Orthotopic SUIT-2 pancreatic tumour and its metastatic nodules in mesentery of mice*

We previously found that NK012 could eradicate human tumour xenografts grown subcutaneously in mice.[19] However, the pathological features of the subcutaneous tumour were different from those of the human pancreatic cancer. Additionally, the latter frequently exhibits extensive invasion into surrounding tissue. To assess the antitumour effects of NK012 in a model similar to human pancreatic cancer, we established orthotopic pancreatic tumour xenografts. We then examined pancreatic tumour growth and spread in the mesentery from 1 to 3 weeks postinjection of SUIT-2 cells into the pancreas (Fig. 2A). The tumour transplanted orthotopically grew from 1 to 3 weeks within the pancreatic body, and thereafter metastatic nodules developed in the mesentery. We also compared the number of blood vessels between an orthotopic tumour and a subcutaneous tumour 3 weeks post-inoculation (Fig. 2B). We found that the orthotopic tumour had a smaller number of blood vessels than the subcutaneous tumour.

3.3. *Antitumour activity of NK012, CPT-11 and gemcitabine against SUIT-2 orthotopic pancreatic tumour xenografts*

Kaplan–Meier analysis showed significant improvement in survival rate in the NK012 treatment group (ILS%, 177) than in the control, CPT-11 (ILS% 63) and gemcitabine groups (ILS%, 74) (Fig. 3A). Regarding antitumour activity, a photon imager indicated that NK012 showed the most potent activity amongst all treatment drugs (Fig. 3B). To confirm the antitumour effects obtained by the photon imager, each tumour was excised for tumour volume and weight measurement (Fig. 3C). NK012 also strongly inhibited the metastatic nodule area compared with the control group (Fig. 3D).

3.4. *Studies on distribution and pharmacokinetics analysis of NK012 and CPT-11 in orthotopic pancreatic tumour tissues*

To examine NK012 and CPT-11 distributions, pancreatic tumour tissues were obtained 1, 6, 24 and 48 h after NK012 or CPT-11 injection, and frozen sections were observed under a fluorescence microscope (Fig. 4A). The drug distribution pattern was clearly different between NK012 and CPT-11. In the sections of CPT-11-treated tumour tissues, fluorescence from CPT-11 was observed in the area of entire tumour tissue, and maximum drug accumulation occurred within 1 h of CPT-11 injection. However, 24 h after CPT-11 injection, fluorescence had almost disappeared and no CPT-11 accumulation was observed thereafter. In the sections of NK012-treated tumour tissues, fluorescence from NK012 started appearing within the tumour tissue 1 h after NK012 injection. The fluorescence area started to increase throughout the tumour tissue 6 h postinjection and maximum fluorescence was observed at 24 h. The fluorescence from NK012 continued to be observed

Please cite this article in press as: Saito Y et al., Antitumour activity of NK012, SN-38-incorporating polymeric micelles, in hypovascular orthotopic pancreatic tumour, *Eur J Cancer* (2009), doi:10.1016/j.ejca.2009.11.014

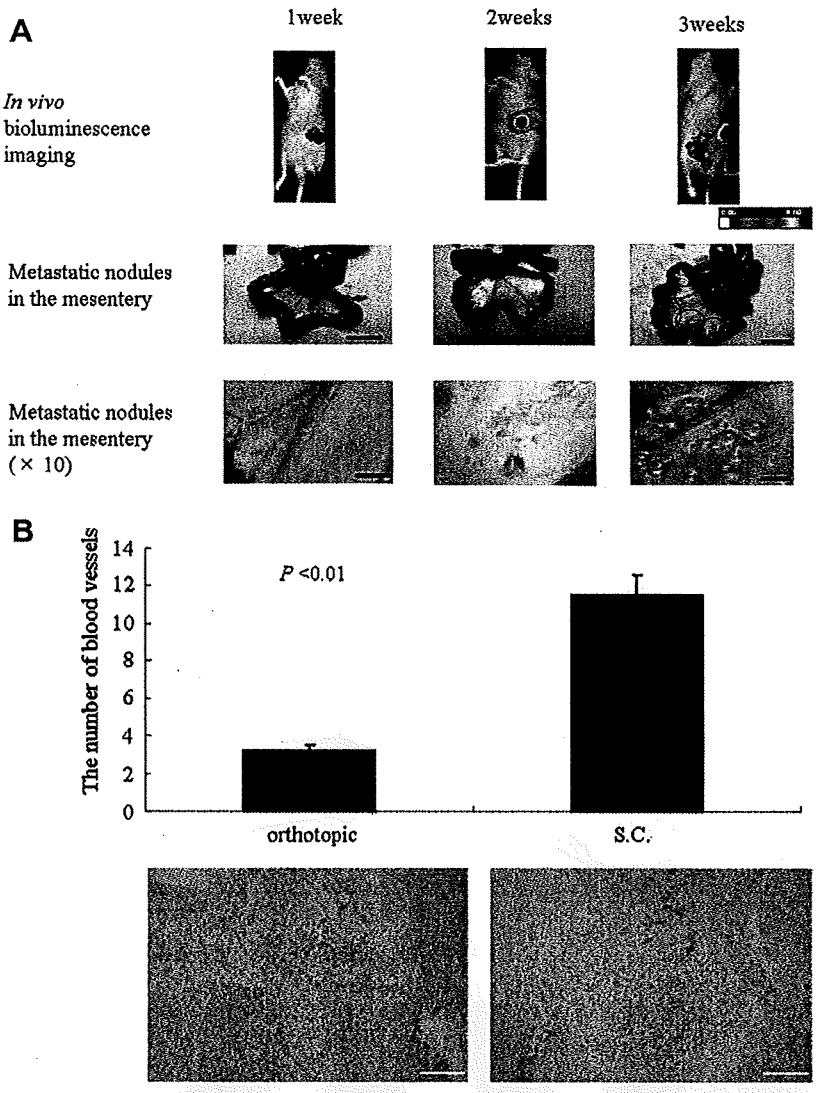

Fig. 2 – Progression of orthotopically implanted SUIT-2 pancreatic tumour xenografts. (A) *In vivo* bioluminescence imaging (upper panels) and metastastic nodules in the mesentery (middle panels: scale bar, 10 mm; lower panels: scale bar, 1 mm). (B) Number of blood vessels in orthotopic tumour xenografts and subcutaneous (S.C.) tumour xenografts. After immunostaining with anti-factor VIII antibody, the number of tumour blood vessels in each xenograft was counted. Column, mean + SD. P < 0.01 (orthotopic versus S.C.). Scale bar: 200 μm.

until 48 h. Microscopic observations were confirmed quantitatively by measuring the amount of SN-38 from tumour tissues by reversed-phase HPLC. In the tumour tissues (Fig. 4B), CPT-11 concentration decreased rapidly with time in a log-liner fashion after CPT-11 injection. Free SN-38 (converted from CPT-11) was only detected 1 h after CPT-11 injection. On the other hand, NK012 (polymer-bound SN-38) and free SN-38 (released from NK012) continued to be detected from 1 to 192 h after NK012 injection. Additionally, we compared NK012 concentration between pancreatic tumour tissues and normal pancreatic tissues (Fig. 4C). NK012 concentration in normal pancreatic tissues was significantly lower than that in pancreatic tumour tissues from 1 to 192 h after NK012 injection.

4. Discussion

Here, we used an orthotopic pancreatic tumour model to evaluate the antitumour effects of NK012. The orthotopic pancreatic cancer xenografts showed poorer vasculature and more abundant interstitium than the subcutaneous tumour xenografts. Moreover, peritoneal dissemination accompanied the orthotopic tumour. These results indicate that SUIT-2 orthotopic tumours can be used as a substitute for locally advanced human pancreatic cancer.

NK012 showed more potent antitumour activity and longer survival rate than CPT-11, gemcitabine and control. We observed drug accumulation and distribution within tumour tissues by fluorescence microscopy. Maximum drug accumulation was observed within 1 h of CPT-11 injection. Twenty-four hours after CPT-11 injection, fluorescence from CPT-11 had almost disappeared, whilst that from NK012 started appearing within the tumour tissues 1 h postinjection, and then spread to the entire body of the pancreatic tumour tissues by 48 h postinjection. These microscopic observations were confirmed quantitatively by HPLC. Regarding the distribution of NK012 in normal major organs, it showed relatively

Please cite this article in press as: Saito Y et al., Antitumour activity of NK012, SN-38-incorporating polymeric micelles, in hypovascular orthotopic pancreatic tumour, *Eur J Cancer* (2009), doi:10.1016/j.ejca.2009.11.014

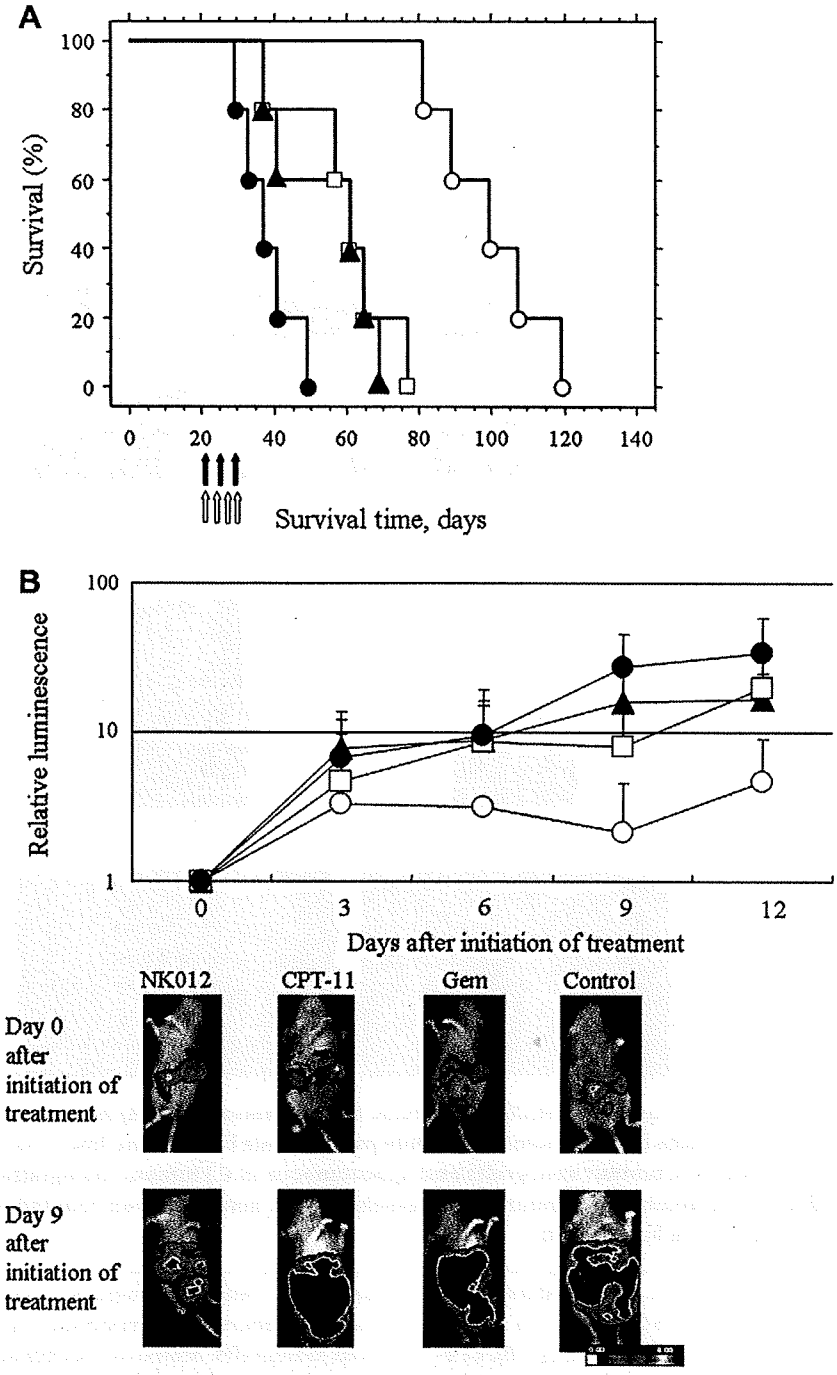

Fig. 3 – Antitumour effects of NK012 in orthotopic tumour xenografts. Mice bearing SUIT-2 tumours were assigned into 4 groups, 21 d after tumour inoculation. Mice were intravenously administered with NK012 (○) (30 mg/kg/d), CPT-11 (▲) (66.7 mg/kg/d) and 0.9% NaCl solution (●) (as a control) on days 0 (21 d after tumour inoculation), 4 and 8. Gemcitabine (□) (16.5 mg/kg/d) was administrated intraperitoneally on days 0, 3, 6 and 9. (A) Effects of NK012 treatment on survival. Survival was assessed by Kaplan–Meier analysis. NK012, CPT-11 and 0.9% NaCl solution were administered on days 0, 4 and 8 (black arrows) and gemcitabine on days 0, 3, 6 and 9 (white arrows). $P < 0.0018$ (NK012 versus CPT-11), $P < 0.0018$ (NK012 versus gemcitabine), $P < 0.0018$ (NK012 versus control). (B) Representative luminescence intensity images obtained in individual control and treatment group mice on days 0 and 9. Points, mean + SD. $P = 0.0074$ (NK012 versus control), $P = 0.0231$ (NK012 versus CPT-11), $P = 0.0239$ (NK012 versus gemcitabine). (C) Tumour volume and tumour weight in mice treated with NK012, CPT-11, gemcitabine and control. Column, mean + SD. $^{*}P < 0.05$ (versus NK012). $^{**}P < 0.01$ (versus NK012). Scale bar, 10 mm. (D) Suppression of metastatic nodules in mesentery by NK012. After 12 d of treatment initiation, the mesentery was dissected and nodule area was measured. Upper panel scale bar, 10 mm; lower panel scale bar, 1 mm. Graph column, mean + SD. $^{**}P < 0.01$ (versus NK012).

Please cite this article in press as: Saito Y et al., Antitumour activity of NK012, SN-38-incorporating polymeric micelles, in hypovascular orthotopic pancreatic tumour, *Eur J Cancer* (2009), doi:10.1016/j.ejca.2009.11.014

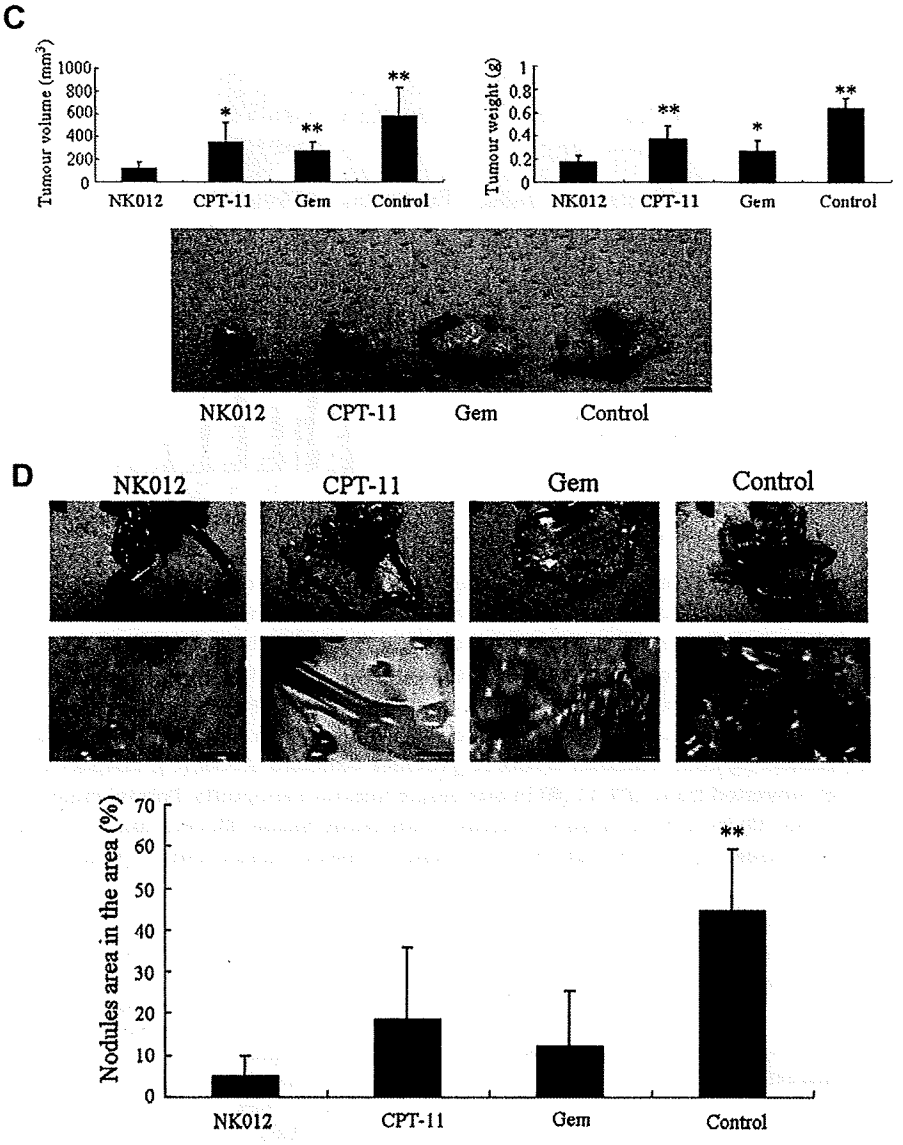

Fig 3. *(continued)*

prolonged distribution in the liver and spleen.[14] However, hepatic toxicity was not observed by a biochemical analysis in the injection of NK012. This long SN-38 retention time is important for its antitumour effects because its antitumour activity is time-dependent.[22] Therefore, we conclude that long-term distribution and retention of NK012 and SN-38 released from NK012 is one of the essential properties underlying the superior antitumour activity of NK012 in such stroma-rich tumours.

In hypervascular tumours, drug formulations categorised in DDS can effectively accumulate in the tumours and sufficiently exert antitumour effect. However, in hypovascular tumours, for example, liposomal drugs can be efficiently delivered to the tumour tissue but free drugs are not sufficiently distributed to cancer cells. Because their formulation is too large to allow penetration of tumour interstitium and is too stable to allow the free drug within liposomes to be released easily. In fact, Doxil[23], a pegylated liposomal doxorubicin, is clinically effective against hypervascular cancers[24,25] such as ovarian tumours, breast cancer and Kaposi sarcoma but not against stomach and pancreatic cancers, both of which have a low density of tumour microvessels. On the other hand, NK012 is small (20 nm)[14] compared with liposomes, which is why it can be distributed more uniformly in the tumour tissue. Furthermore, NK012 has the potential to allow the effective sustained release of free SN-38 inside a tumour following NK012 accumulation in the tumour tissue. Consequently, SN-38 thus released distributes throughout the tumour tissue and is internalised into cancer cells to kill them.

Here, we have shown that NK012 has potent antitumour effects against orthotopic pancreatic tumours compared with gemcitabine and CPT-11, and that NK012 decreased the number of metastatic nodules in the peritoneal cavity. Thus, we admonish that it is better to use orthotopic tumour xenografts to evaluate the antitumour activity against cancer characterised by few tumour vessels and high amount of tumour stroma. Moreover, enhanced accumulation, distribution and retention of polymeric micelle-based anticancer drugs within the tumour tissue and the sustained release of anticancer drugs from the micelles are key elements for the treatment

Please cite this article in press as: Saito Y et al., Antitumour activity of NK012, SN-38-incorporating polymeric micelles, in hypovascular orthotopic pancreatic tumour, *Eur J Cancer* (2009), doi:10.1016/j.ejca.2009.11.014

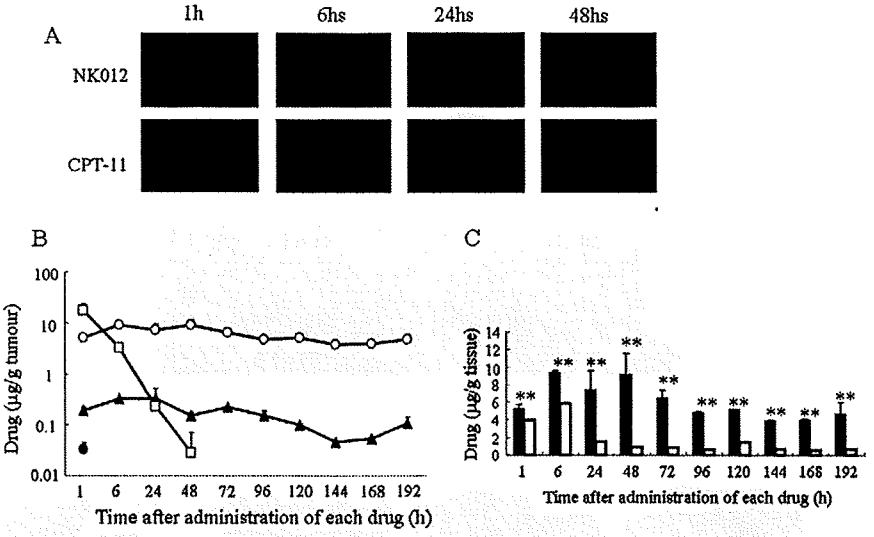

Fig. 4 – Distribution of NK012 or CPT-11 in orthotopic tumour xenografts. Concentrations of NK012 (polymer-bounded SN-38), free SN-38 and CPT-11 in tumour or normal pancreatic tissues. (A) Mice bearing SUIT-2 tumours were injected with NK012 (30 mg/kg) or CPT-11 (66.7 mg/kg). Tumour tissues were excised 1, 6, 24 and 48 h after intravenous NK012 or CPT-11. Each mouse was administered with fluorescein-labelled *Lycopersicon esculentum* lectin 5 min before sacrifice to detect tumour blood vessels. Frozen tissue sections were examined under a fluorescence microscope at an excitation wavelength of 377 nm and an emission wavelength of 477 nm. The same fluorescence condition can be applied for visualising NK012 and CPT-11 fluorescence. Scale bar, 100 μm. (B) Concentration of NK012 (polymer-bounded SN-38) (○), free SN-38 released from NK012 (▲), CPT-11 (□) and free SN-38 converted from CPT-11 (●) in orthotopic tumour xenografts. Points, mean + SD. (C) Concentration of NK012 (polymer-bounded SN-38) in tumour tissue or normal pancreatic tissue. Black column, tumour tissues, mean; white column, normal pancreatic tissue, mean. Bar, SD. **P < 0.01 (tumour tissue versus normal pancreas, each time).

of hypovascular tumours. A phase I clinical trial of NK012 has been completed.[26,27] A future phase II clinical trial in patients with hypovascular and stroma-rich tumour such as pancreatic cancer is warranted.

Conflict of interest statement

None declared.

Acknowledgements

The authors declared no potential conflict of interest. This work was supported partly by a Grant-in-Aid from the Third Term Comprehensive Control Research for Cancer, the Ministry of Health, Labour and Welfare (Matsumura, H19-025), Scientific Research on Priority Areas from the Ministry of Education, Culture, Sports, Science and Technology (Matsumura, 17016087), and Japanese Foundation for Multidisciplinary Treatment of Cancer (Matsumura) and the Princess Takamatsu Cancer Research Fund (07-23908). We thank N. Mie, M. Ohtsu and Y. Hashimoto for their technical assistance and K. Shiina for her secretarial assistance.

REFERENCES

1. Jemal A, Siegel R, Ward E, et al. Cancer statistics, 2008. *CA Cancer J Clin* 2008;58:71–96.
2. Warshaw AL, Fernández-del Castillo C. Pancreatic carcinoma. *N Engl J Med* 1992;326:455–65.
3. Wanebo HJ, Vezeridis MP. Pancreatic carcinoma in perspective. A continuing challenge. *Cancer* 1996;78:580–91.
4. Casper ES, Green MR, Kelsen DP, et al. Phase II trial of gemcitabine (2,2′-difluorodeoxycytidine) in patients with adenocarcinoma of the pancreas. *Invest New Drugs* 1994;12:29–34.
5. Carmichael J, Fink U, Russell RC, et al. Phase II study of gemcitabine in patients with advanced pancreatic cancer. *Br J Cancer* 1996;73:101–5.
6. Moore MJ, Goldstein D, Hamm J, et al. Erlotinib plus gemcitabine compared with gemcitabine alone in patients with advanced pancreatic cancer: a phase III trial of the National Cancer Institute of Canada Clinical Trials Group. *J Clin Oncol* 2007;25:1960–6.
7. Hosoki T. Dynamic CT of pancreatic tumors. *AJR Am J Roentgenol* 1983;140:959–65.
8. Sofuni A, Iijima H, Moriyasu F, et al. Differential diagnosis of pancreatic tumors using ultrasound contrast imaging. *J Gastroenterol* 2005;40:518–25.
9. Matsumura Y, Maeda H. A new concept for macromolecular therapeutics in cancer chemotherapy: mechanism of tumoritropic accumulation of proteins and the antitumor agent smancs. *Cancer Res* 1986;46:6387–92.
10. Li LH, Fraser TJ, Olin EJ, Bhuyan BK. Action of camptothecin on mammalian cells in culture. *Cancer Res* 1972;32:2643–50.
11. Gallo RC, Whang-Peng J, Adamson RH. Studies on the antitumor activity, mechanism of action, and cell cycle effects of camptothecin. *J Natl Cancer Inst* 1971;46:789–95.
12. Gottlieb JA, Guarino AM, Call JB, Oliverio VT, Block JB. Preliminary pharmacologic and clinical evaluation of camptothecin sodium (NSC-100880). *Cancer Chemother Rep* 1970;54:461–70.

13. Muggia FM, Creaven PJ, Hansen HH, Cohen MH, Selawry OS. Phase I clinical trial of weekly and daily treatment with camptothecin (NSC-100880): correlation with preclinical studies. *Cancer Chemother Rep* 1972;**56**:515–21.
14. Koizumi F, Kitagawa M, Negishi T, et al. Novel SN-38-incorporating polymeric micelles, NK012, eradicate vascular endothelial growth factor-secreting bulky tumors. *Cancer Res* 2006;**66**:10048–56.
15. Sumitomo M, Koizumi F, Asano T, et al. Novel SN-38-incorporated polymeric micelle, NK012, strongly suppresses renal cancer progression. *Cancer Res* 2008;**68**:1631–5.
16. Nakajima TE, Yasunaga M, Kano Y, et al. Synergistic antitumor activity of the novel SN-38-incorporating polymeric micelles, NK012, combined with 5-fluorouracil in a mouse model of colorectal cancer, as compared with that of irinotecan plus 5-fluorouracil. *Int J Cancer* 2008;**122**:2148–53.
17. Nakajima TE, Yanagihara K, Takigahira M, et al. Antitumor effect of SN-38-releasing polymeric micelles, NK012, on spontaneous peritoneal metastases from orthotopic gastric cancer in mice compared with irinotecan. *Cancer Res* 2008;**68**:9318–22.
18. Kuroda JI, Kuratsu JI, Yasunaga M, Koga Y, Saito Y, Matsumura Y. Potent antitumor effect of SN-38-incorporating polymeric micelle, NK012, against malignant glioma. *Int J Cancer* 2009;**124**:2505–11.
19. Saito Y, Yasunaga M, Kuroda J, Koga Y, Matsumura Y. Enhanced distribution of NK012, a polymeric micelle-encapsulated SN-38, and sustained release of SN-38 within tumors can beat a hypovascular tumor. *Cancer Sci* 2008;**99**:1258–64.
20. Koppe MJ, Oyen WJ, Bleichrodt RP, Verhofstad AA, Goldenberg DM, Boerman OC. Combination therapy using gemcitabine and radioimmunotherapy in nude mice with small peritoneal metastases of colonic origin. *Cancer Biother Radiopharm* 2006;**21**:506–14.
21. Yang HM, Reisfeld RA. Doxorubicin conjugated with a monoclonal antibody directed to a human melanoma-associated proteoglycan suppresses the growth of established tumor xenografts in nude mice. *Proc Natl Acad Sci USA* 1988;**85**:1189–93.
22. Kawato Y, Aonuma M, Hirota Y, Kuga H, Sato K. Intracellular roles of SN-38, a metabolite of the camptothecin derivative CPT-11, in the antitumor effect of CPT-11. *Cancer Res* 1991;**51**:4187–91.
23. Muggia FM. Liposomal encapsulated anthracyclines: new therapeutic horizons. *Curr Oncol Rep* 2001;**3**:156–62.
24. Hassan M, Little RF, Vogel A, et al. Quantitative assessment of tumor vasculature and response to therapy in kaposi's sarcoma using functional noninvasive imaging. *Technol Cancer Res Treat* 2004;**3**:451–7.
25. Emoto M, Udo T, Obama H, Eguchi F, Hachisuga T, Kawarabayashi T. The blood flow characteristics in borderline ovarian tumors based on both color Doppler ultrasound and histopathological analyses. *Gynecol Oncol* 1998;**70**:351–7.
26. Kato K, Hamaguchi T, Shirao K et al. Interim analysis of phase I study of NK012, polymer micelle SN-38, in patients with advanced cancer. *Proc Am Soc Clin Oncol GI 2008* [Abs #485].
27. Burris HA III, Infante JR, Spigel DR, et al. A phase I dose-escalation study of NK012. *Proc Am Soc Clin Oncol 2008* [Abs #2358].

Please cite this article in press as: Saito Y et al., Antitumour activity of NK012, SN-38-incorporating polymeric micelles, in hypovascular orthotopic pancreatic tumour, *Eur J Cancer* (2009), doi:10.1016/j.ejca.2009.11.014